Two Methods for the Calculation of CSR Fields

M. Dohlus

Deutsches Elektronen Synchrotron, DESY, Hamburg, Germany

Abstract

Two methods for the calculation of fields of three dimensional charge distributions on general trajectories are described. Although the source functions are three dimensional, the numerical field calculation is reduced to one-dimensional integrals that have to be evaluated numerically. The first method determines the longitudinal electric field of charge densities that can be factorized into arbitrary longitudinal and transverse distributions. The field is split into a 'linear-motion-part' that is independent of the shape of the general trajectory and a second part, that is under certain conditions, independent on the transverse density function. A special case of this method is the 'small-angle-approach' described in [1]. The second method allows the complete field calculation (electromagnetic fields and potentials) of spherical Gaussian distributions without further restrictions. A generalization for general Gaussian distributions is proposed. A couple of examples demonstrate the applicability of these approaches.

1. Introduction

Very short bunches with high peak currents are required in X-ray Free Electron Lasers (SASE-FELs). In most designs, short bunches are produced by longitudinal compression in magnetic chicanes, where particles with different energies have different path lengths so that a bunch with an energy distribution correlated with longitudinal particle position can shrink in length. However, care has to be taken so that the low emittance beams are not blown up by the electromagnetic self-fields

caused by the bunch. Two types of approaches are presently used to calculate the dynamics of such bunches selfconsistently.

The one-dimensional approach of Borland [2] uses a simplified model for the calculation of longitudinal forces. It neglects transverse beam dimensions and calculates the longitudinal self-field of a one-dimensional beam that is obtained by a projection of the 'real' three-dimensional beam to a reference trajectory. As the field of a one-dimensional beam is infinite on its trajectory a 'renormalized Coulomb' term is used [1]. (This is equivalent to neglecting the 'linear motion' term that is discussed later.) For the field calculation at a certain instant, it is assumed that the longitudinal distribution is ridged and has not changed at retarded times. Transverse self-forces are neglected completely. The field calculation method discussed in section 2 is suited for this approach. The starting point is the description of a three-dimensional source distribution and its predefined motion with respect to a general three-dimensional path. Formally the scalar and vector potential as well as the electromagnetic fields can be expressed as three-dimensional integrals of retarded sources. To find a one-dimensional integral expression for the longitudinal electric field on the reference trajectory we split it artificially into two contributions $\tilde{\tilde{E}}$ and E_l, with E_l the longitudinal field of the same distribution in linear motion. This splitting extracts almost all contributions to $\tilde{\tilde{E}}$ from retarded sources close to the observer. $\tilde{\tilde{E}}$ is represented as the sum of three terms E_1, E_2 and E_3 that can be approximated by one-dimensional integrals if the near effects are negligible. A further simplification is possible for observation positions that are enclosed by trajectories with constant or nearly constant curvature. For such points the 'small angle approximation' [1] and its generalization for arbitrary three-dimensional trajectories are derived. The disadvantage of the 'small angle approximation' and its generalization is that an implicit equation for the retarded time has to be solved for all points of the integration interval. This is avoided by an alternative formulation that uses a substitution for the integration variable.

For self-consistent tracking with the sub-bunch approach [3, 4] the particle distribution is described by a set of sub-bunches. These sub-bunches have a well-defined shape (e.g. Gaussian, time-independent) and each of the sub-bunches has an individual trajectory that is known for the past. This defines the source distribution

$\rho(\mathbf{r},t)$ so that potentials and electromagnetic fields can be calculated by an integration of the retarded sources. The field calculation in [5] is directly based on the Liénard Wiechert equations. A disadvantage of the sub-bunch approach is the large numerical effort. For N observer particles and M field generating bunches $N \times M$ three-dimensional integrations have to be performed for every time step. The effort can be reduced considerably by more efficient field calculations for sub-bunches [6], by the simultaneous integration of all sources and by an improved and more flexible generation of the set of sub-bunches. In section 3 a method is decribed to calculate electromagnetical fields of spherical Gaussian sub-bunches by a one-dimensional integration without any approximations and a generalization for arbitrary Gaussian distributions is proposed.

2. Longitudinal Field of Bunches with Arbitrary Longitudinal Profile

2.1. Source and Observer

To describe the three-dimensional source distributions $\rho(\mathbf{r},t)$ a one-dimensional "longitudinal" density function $\lambda(s)$ with the bunch charge $q = \int \lambda ds$ and a two dimensional density function $\eta(x_1, x_2)$ with $\int \eta dx_1 dx_2 = 1$ are defined. Further we define a general three-dimensional trajectory $\mathbf{r}_s(\hat{s})$ and a plane $\mathbf{r}_\eta(x_1, x_2) = x_1\mathbf{u}_1 + x_2\mathbf{u}_2$ with $\hat{s}$ the length coordinate, $\mathbf{u}_s(\hat{s}) = \partial_{\hat{s}}\mathbf{r}_s(\hat{s})$ the unity vector in tangential direction, $\mathbf{u}_1 \cdot \mathbf{u}_2 = 0$ and $\mathbf{u}_3 = \mathbf{u}_1 \times \mathbf{u}_2$ the normal vector to the $\mathbf{r}_\eta$-plane. The line charge denisty of a beam without transverse dimensions and with constant velocity $v = \beta c$ along the trajectory is $\lambda(\hat{s} - vt)$. A certain type of three-dimensional charge density is obtained by the convolution of the line charge density $\lambda(\hat{s} - vt)$ and the two-dimensional density $\eta(x_1, x_2)$ with respect to their three dimensional allocation $\mathbf{r}_s(\hat{s})$ and $\mathbf{r}_\eta(x_1, x_2)$. This charge density is formally descibed by

$$\rho\big(\mathbf{r}_s(\hat{s}) + \mathbf{r}_\eta(x_1, x_2), t\big)\det\big(\mathbf{u}_1, \mathbf{u}_2, \mathbf{u}_s(\hat{s})\big) = \lambda(\hat{s} - vt)\eta(x_1, x_2)\,. \qquad (1)$$

In the following we assume that the angle between the path direction $\mathbf{u}_s(\hat{s})$ and the normal vector $\mathbf{u}_3$ is small, so that x_1, x_2 are approximately transverse coordinates and $\eta(x_1, x_2)$ is approximately the transverse denisty. The typical longitudinal and

transverse dimensions of the beam are characterized by σ_λ and σ_η (e.g. rms dimensions). Δ_λ and Δ_η are maximal dimensions with $\lambda(s) = 0$ and $\eta(x_1, x_2)$ =0 for $|s| > \Delta_\lambda$ and $x_1^2 + x_2^2 > \Delta_\eta^2$.

The longitudinal electric field is calculated for an observer that travels *on* the trajectory. Therefore the position and longitudinal direction of the observer are defined by the longitudinal coordinate s_o as $\mathbf{r}_o = \mathbf{r}_s(s_o)$ and $\mathbf{u}_o = \mathbf{u}_s(s_o)$.

2.2. Scalar- and Vector-Potential

The electromagnetic fields are derived from the scalar and vector potential for Lorentz gauge. The three-dimensional integration of the retarded sources defined by Eq. (1) results in:

$$4\pi\varepsilon\Phi(\mathbf{r},t) = \int \frac{\rho(\mathbf{r}',t')}{\|\mathbf{r}-\mathbf{r}'\|} dV' = \int \frac{\lambda(s+s_o-vt')\eta(x_1,x_2)}{R(\mathbf{r},s+s_o,x_1,x_2)} dx_1 dx_2 ds \ , \qquad (2a)$$

$$\begin{aligned} 4\pi\varepsilon\mathbf{A}(\mathbf{r},t) &= c^{-2} \int \frac{\mathbf{J}(\mathbf{r}',t')}{\|\mathbf{r}-\mathbf{r}'\|} dV' \\ &= \beta c^{-1} \int \frac{\lambda(s+s_o-vt')\eta(x_1,x_2)}{R(\mathbf{r},s+s_o,x_1,x_2)} \mathbf{u}_s(s+s_o) dx_1 dx_2 ds \end{aligned} \ , \qquad (2b)$$

with the vectorial and scalar distance functions

$$\begin{aligned} \mathbf{R}(\mathbf{r},\hat{s},x_1,x_2) &= \mathbf{r} - \mathbf{r}_s(\hat{s}) - \mathbf{r}_\eta(x_1,x_2) \\ R(\mathbf{r},\hat{s},x_1,x_2) &= \|\mathbf{R}(\mathbf{r},\hat{s},x_1,x_2)\| \end{aligned} \ ,$$

and the retarded time $t' = t - c^{-1}\|\mathbf{r}-\mathbf{r}'\| = t - c^{-1}R(\mathbf{r},\hat{s},x_1,x_2)$. This is equivalent to the convolution of the line charge potentials $\Phi^{(\lambda)}(\mathbf{r},t)$ and $\mathbf{A}^{(\lambda)}(\mathbf{r},t)$ with the transverse density function $\eta(x_1,x_2)$:

$$\begin{aligned} \Phi(\mathbf{r},t) &= \Phi^{(\lambda)}(\mathbf{r},t) \otimes \eta(x_1,x_2) \\ \mathbf{A}(\mathbf{r},t) &= \mathbf{A}^{(\lambda)}(\mathbf{r},t) \otimes \eta(x_1,x_2) \end{aligned} \ . \qquad (3)$$

The convolution operator is defined by

$$X(\mathbf{r},t) \otimes \eta(x_1,x_2) = \int X(\mathbf{r} - \mathbf{r}_\eta(x_1,x_2))\eta(x_1,x_2) dx_1 dx_2 \ ,$$

and the potentials of the line charge source are calculated by a one-dimensional integration equivalent to Eq. (2):

$$4\pi\varepsilon\Phi^{(\lambda)}(\mathbf{r},t) = \int \frac{\lambda(s+s_o-vt')}{R^{(\lambda)}(\mathbf{r},s+s_o)}ds\,, \tag{4a}$$

$$4\pi\varepsilon\mathbf{A}^{(\lambda)}(\mathbf{r},t) = \beta c^{-1}\int \frac{\lambda(s+s_o-vt')}{R^{(\lambda)}(\mathbf{r},s+s_o)}\mathbf{u}_s(s+s_o)ds\ . \tag{4b}$$

with $R^{(\lambda)}(\mathbf{r},\hat{s}) = \left\|\mathbf{r}-\mathbf{r}_s(\hat{s})\right\|$ and $t' = t - c^{-1}R^{(\lambda)}(\mathbf{r},\hat{s})$.

A few words on notation: all unspecified integration ranges are infinite. For the rest of the report we skip the arguments of functions in the integrals and use the following notation (unless specified differently):

$$\begin{aligned}
&\mathbf{r}_s = \mathbf{r}_s(s+s_o)\\
&\mathbf{u}_s = \mathbf{u}_s(s+s_o)\\
&\mathbf{R} = \begin{cases}\mathbf{r}_o-\mathbf{r}_s-\mathbf{r}_\eta(x_1,x_2) & \text{in 3d integrals}\\ \mathbf{r}_o-\mathbf{r}_s & \text{in 1d integrals}\end{cases}\\
&R = \|\mathbf{R}\|\\
&\mathbf{n} = \mathbf{R}/R\\
&t' = t - c^{-1}R\\
&\lambda = \lambda(s+s_o-vt')
\end{aligned}$$

The longitudinal interval with non-vanishing retarded sources in Eqs. (2, 4) is implicitly defined by:

$$-\Delta_\lambda < s+s_o-vt' = s+\beta\left\|\mathbf{r}_o-\mathbf{r}_s(s+s_o)\right\|+s_o-vt < \Delta_\lambda\ . \tag{5}$$

For simplicity we neglect transverse beam dimensions. To provide insight into typical interaction lengths, we estimate the path length difference $L_\lambda = |s|$ between the observer particle (at s_o) and the retarded position of a source particle that is σ_λ behind. This is the solution of $s+\beta\left\|\mathbf{r}_o-\mathbf{r}_s(s+s_o)\right\| = -\sigma_\lambda$. The distance functions for linear motion and for circular motion with curvature radius R_0 are:

$$\left\|\mathbf{r}_o-\mathbf{r}_s(s+s_o)\right\| = \begin{cases}|s| & \text{for linear motion}\\ \left|2R_0\sin\left(\dfrac{s}{2R_0}\right)\right| & \text{for circular motion}\end{cases},$$

and L_λ follows as

$$L_\lambda = \begin{cases} \sigma_\lambda/(1-\beta) & \text{for linear motion} \\ \sqrt[3]{24R_0^2\sigma_\lambda} & \text{for circular motion} \end{cases} . \qquad (4)$$

The solution for circular motion is an approximation and is valid if $L_\lambda << R_0$ and $(1-\beta)L_\lambda << \sigma_\lambda$. For example for a bunch with the length $\sigma_\lambda = 100\mu$m in a bunch compressor with bending radii $R_0 = 10$ m, the typical interaction length is *at least* $\sqrt[3]{24R_0^2\sigma_\lambda} \approx 0.62$ m. For observers *in* the bunch ($|s_o - vt| < \Delta_\lambda$) the interaction length with *head* particles ($\propto \sigma_\lambda$) is usually much shorter than with tail particles. However the main contribution to the longitudinal electric field comes from the negative part of the integration range.

2.3. Longitudinal Electric Field

The longitudinal electric field $E_\parallel$ observed by a test particle with the velocity $\mathbf{v}$ can be expressed as:

$$E_\parallel v = \mathbf{E}\cdot\mathbf{v} = -\nabla\Phi\cdot\mathbf{v} - \partial_t\mathbf{A}\cdot\mathbf{v} = -d_t\Phi + \partial_t(\Phi - \mathbf{A}\cdot\mathbf{v}) , \qquad (6)$$

with $d_t = d/dt$ and $\partial_t = \partial/\partial t$. This can be split into the three terms

$$\begin{aligned} E_1 &= -v^{-1}d_t\Phi \\ E_2 &= v^{-1}\partial_t(\beta^2\Phi - \mathbf{A}\cdot\mathbf{v}) , \\ E_\gamma &= v^{-1}\gamma^{-2}\partial_t\Phi \end{aligned} \qquad (7)$$

with $\gamma = 1/\sqrt{1-\beta^2}$. There are two mathematical and one physical reason for this splitting: the integrals of the first two terms converge even for one-dimensional distributions, the first two terms are dominated by long range interactions with retarded sources, and the third term is proportional to γ^{-2} for source distributions with $\sigma_\lambda >> R_c/\gamma^3$ with R_c the curverture radius of the trajectory.

In the following we show that E_1 and E_2 can be approximated by one-dimensional integrals. To use a similar technique for at least a part of the last term, we split E_γ into a 'linear motion' term E_l and a residual term E_3:

$$E_3 = v^{-1}\gamma^{-2}\partial_t\left(\Phi - \Phi_l\right)$$
$$E_l = v^{-1}\gamma^{-2}\partial_t\Phi_l \qquad (8)$$

E_l and Φ_l are the longitudinal field and the scalar potential of the source distribution for motion along a linear path $\mathbf{r}_l(\hat{s}) = \mathbf{r}_o + \mathbf{u}_o(\hat{s} - s_o)$ that is tangential to the (general) trajectory at $\mathbf{r}_s(\hat{s})$. In this report we discuss the calculation of the terms E_1, E_2 and E_3, but not the 'linear motion' term E_l that is proportional to γ^{-2} and behaves as expected for distributions in uniform linear motion.

2.4. Integral Representation of E_1, E_2 and E_3

The integral representations of the terms E_1, E_2 and E_3 in Eqs. (7) and (8) are

$$4\pi\varepsilon E_1 = \int\left(\frac{\lambda}{R^2} - \frac{\beta\lambda'}{R}\right)\mathbf{n}\cdot\left(\mathbf{u}_o - \mathbf{u}_s\right)\eta\, dx_1 dx_2 ds \quad , \qquad (9a)$$

$$4\pi\varepsilon E_2 = -\beta^2\int\frac{\lambda'}{R}(1 - \mathbf{u}_s(s)\cdot\mathbf{u}_o)\eta\, dx_1 dx_2 ds \quad , \qquad (9b)$$

$$4\pi\varepsilon E_3 = \gamma^{-2}\int\left(-\frac{\lambda'}{R} + \frac{\lambda_l'}{R_l}\right)\eta dx_1 dx_2 ds \qquad (9c)$$

with

$$\mathbf{n} = \mathbf{R}\left(\mathbf{r}, s + s_o, x_1, x_2\right)/R\left(\mathbf{r}, s + s_o, x_1, x_2\right)$$
$$R_l = \sqrt{s^2 + x_1^2 + x_2^2} \qquad .$$
$$\lambda_l = \lambda\left(s + \beta R_l + s_o - vt\right)$$

For the first term E_1 we calculated the total derivative of Eq. (2a), using $\nabla R = \mathbf{n}$ and an integration by parts:

$$\int\frac{d}{ds}\left(\frac{\lambda}{R}\right)ds = \int\frac{\partial\lambda}{\partial s}\frac{1}{R}ds + \int\frac{\partial}{\partial R}\left(\frac{\lambda}{R}\right)\frac{dR}{ds}ds = 0 \quad .$$

The second and third term E_2 and E_3 follow directly from the partial derivative of Eqs. (2a) and (2b) and an integral formulation of the 'linear motion' potential

$$4\pi\varepsilon\Phi_l(\mathbf{r}, t) = \int\frac{\lambda_l\eta}{R_l}dx_1 dx_2 ds$$

that is analogue to Eq. (2a).

To approximate the three-dimensional integrals in Eq. (9) by a one-dimensional integration along the s coordinate we have to investigate the dependency of the integrands on the transverse coordinates x_1 and x_2. The integrands are a product of the transverse distribution function $\eta(x_1, x_2)$ (with $\int \eta dx_1 dx_2 = 1$) and terms that depend on the distance function $R(\mathbf{r}, \hat{s}, x_1, x_2)$. For large values of $|s|$, the distance function $R(\mathbf{r}, \hat{s}, x_1, x_2)$ can be approximated by:

$$R(\mathbf{r}, \hat{s}, x_1, x_2) \approx R(\mathbf{r}, \hat{s}, 0, 0) - \mathbf{r}_\eta(x_1, x_2) \cdot \mathbf{n}(\mathbf{r}, s, 0, 0) + \frac{\left\| \mathbf{r}_\eta(x_1, x_2) \right\|^2}{2R(\mathbf{r}, s, 0, 0)} \ .$$

The x_1, x_2 dependency of the distance function is negligible for $x_1^2 + x_2^2 < \Delta_\lambda^2$ if the distance $R \approx |s|$ is large and the offset dependency $R(\mathbf{r}, \hat{s}, x_1, x_2) - R(\mathbf{r}, \hat{s}, 0, 0)$ small compared to the bunch length σ_λ. This is equivalent to the conditions

$$\begin{aligned} &|s| >> \Delta_\lambda \\ &|s| >> \Delta_\eta^2 / \Delta_\lambda \\ &\Delta_\lambda / \Delta_\eta >> \mathbf{u}_3 \cdot \mathbf{n}(\mathbf{r}, s, 0, 0) \end{aligned} \quad . \tag{10}$$

As we made the assumption $\mathbf{u}_3 \cdot \mathbf{u}_s(s) \approx 1$ in the beginning, the last criterion is always fulfilled for beams with not too extremean aspect ratio $\sigma_\eta / \sigma_\lambda$. The s integration range is split into a part where condition (10) is fullfilled (part a) and the rest (part b). Therefore we can simplify the integration of part a: $\int_{\text{part a}} \cdots \eta dx_1 dx_2 ds \approx \int_{\text{part a}} \cdots ds$, and roughly estimate part b: $\int_{\text{part b}} \cdots \eta dx_1 dx_2 ds \approx \int_{\text{part b}} \cdots ds$. If the total integral is dominated by long range interactions so that the criterion

$$\left| \int_{\text{part b}} \cdots ds \right| \approx \left| \int_{\text{part b}} \cdots \eta dx_1 dx_2 ds \right| << \left| \int_{\text{part a}} \cdots ds \right| \tag{11}$$

is fulfilled, the longitudinal electric field (without 'linear motion' part) can be calculated by one-dimensional integration:

$$4\pi\varepsilon E_1 = \int \left(\frac{\lambda}{R^2} - \frac{\beta\lambda'}{R} \right) \mathbf{n} \cdot \left(\mathbf{u}_o - \mathbf{u}_s \right) ds \,, \tag{12a}$$

$$4\pi\varepsilon E_2 = -\beta^2 \int \frac{\lambda'}{R}(1-\mathbf{u}_s\cdot\mathbf{u}_o)ds\,, \tag{12b}$$

$$4\pi\varepsilon E_3 = \gamma^{-2}\int\left(-\frac{\lambda'}{R}+\frac{\lambda_l'}{R_l}\right)ds\,. \tag{12c}$$

Formally the same result could be obtained for a one-dimensional beam, but it has to be noted that transverse field components and E_l are infinite.

For observer positions in the bunch or ahead ($s_o > vt - \Delta_\lambda$) criterion (11) is usually fulfilled. This is obvious for trajectories that are linear in the neighborhood of the observer and it will be shown later for circular trajectories.

2.5. More about E_1

To find a uniform expression for $\tilde{E} = E - E_l = E_1 + E_2 + E_3$ we want to neglect the term λ/R^2 in the integrand of Eq. (12a) so that

$$4\pi\varepsilon E_1 = -\beta\int\frac{\lambda'}{R}\mathbf{n}\cdot(\mathbf{u}_o-\mathbf{u}_s)ds\,. \tag{13}$$

This is justified by the following arguments.

a) Stationary trajectories: For linear, circular and helical trajectories the factor $\mathbf{n}\cdot(\mathbf{u}_o-\mathbf{u}_s)$ is zero and λ/R^2 does not contribute (as well as λ'/R). For this type of trajectory the scalar potential is a stationary function, its total derivative is zero and the term E_1 vanishes. It has to be emphasized that this is fulfilled only for the particular choice of the observer position $\mathbf{r}_o = \mathbf{r}_s(s_o)$ and direction $\mathbf{u}_o = \mathbf{u}_s(s_o)$. For observers with constant offset to the trajectory and for circular or helical motion there is a relative motion in the restframe that causes a change of the potential (compare Fig. 2).

b) Locally stationary trajectories: If a trajectory is linear, circular or helical in the neighbourhood of the observation position the integation range of (12b) can be split into a stationary part (around the observer) and the rest. The stationary part does not contribute and for the rest the approximation $\beta\lambda'/R - \lambda/R^2 = \partial_R(\lambda R^{-1}) \approx \beta\lambda' R^{-1}$ is used. This approximation is appropriate if the distance $|s_o - s_t|$ between the observer

and transition points (at $\hat{s} = s_t$) is large compared to the bunchlength Δ_λ. Therefore the full range integration Eq. (13) can be used for all observation positions with stationary trajectories in the close surrounding. The criterion $|s_o - s_t| >> \Delta_\lambda$ is still too strict, as one finds from analysis of the arc to line and line to arc transitions. It can be shown that $\int(\lambda/(4\pi\varepsilon R^2))\mathbf{n}\cdot(\mathbf{u}_o - \mathbf{u}_s)ds$ scales as

$$-0.016\frac{q_0}{\varepsilon}\frac{s_o}{\sigma_\lambda R_0^2}\begin{cases}1 - s_o/L_\lambda + \ln(s_o/L_\lambda) & \text{transition from arc to line}\\ (1-s_o/L_\lambda)^2/2 & \text{transition from line to arc}\end{cases}$$

for an observer position s_o after the transition at $s_t = 0$, with R_0 the curvature radius and L_λ the typical interaction length (compare Eq. (5)). This is usually negligible compared to the steady state field of a bunch in circular motion (compare Eq. (19) that will be derived later).

c) Trajectories with continuous curvature: The scalar product in Eq. (12a) is estimated by the lowest order Taylor expansion arround the observation point:

$$\mathbf{n}\cdot(\mathbf{u}_o - \mathbf{u}_s) = -\frac{K(s_o)K'(s_o)}{12}|s|^3 + O(s^4).$$

The path function has to be sufficiently smooth, so that the first derivative of the curvature function $K(\hat{s}) = \|\partial_{\hat{s}}\mathbf{u}_s(\hat{s})\|$ exists. The integral for E_1 follows with $R \approx |s|$ as

$$\int\left(\frac{\lambda}{R^2} - \frac{\beta\lambda'}{R}\right)\mathbf{n}\cdot(\mathbf{u}_o - \mathbf{u}_s)ds \approx -\frac{KK'}{12}\int(\lambda|s| - \beta\lambda' s^2)ds.$$

The negative part of the integration range has a length of the order of L_λ and is (usually) much longer than the positive part $\propto \sigma_\lambda$ and the bunch. Therefore the λ' term contributes much more than the λ term.

2.6. Simplified One-Dimensional Integral

Eqs. (12b,c) and (13) are combined to one expression for $\tilde{E} = E - E_l$ and the λ_l'/R_l term is modified by the use of the substitution $s + \beta R_l(s) = u + \beta R(u)$ so that an integral expression is found that depends on $\lambda' = \lambda'(s + \beta R + s_o - vt)$ and the kernel $K(s_o, s)$:

$$4\pi\varepsilon\tilde{E} = 4\pi\varepsilon(E - E_l) = \int \lambda' \cdot K(s_o, s)ds$$
$$K(s_o, s) = \frac{\beta\mathbf{n}\cdot(\mathbf{u}_s - \mathbf{u}_o) - \beta^2(1 - \mathbf{u}_s\cdot\mathbf{u}_o) - \gamma^{-2}}{R} + \frac{1 - \beta\mathbf{u}_s\cdot\mathbf{n}}{\gamma^2|s + \beta R|} \tag{14a}$$

An equivalent expression that depends on $\lambda'(u + s_o - vt)$ follows from the substitution $u = s + \beta R(s)$:

$$4\pi\varepsilon\tilde{E} = \int \lambda'(u + s_o - vt)\cdot\tilde{K}(s_o, u)du$$
$$\tilde{K}(s_o, u) = \left(\frac{\beta\mathbf{n}\cdot(\mathbf{u}_s - \mathbf{u}_o) - \beta^2(1 - \mathbf{u}_s\cdot\mathbf{u}_o) - \gamma^{-2}}{R(1 - \beta\mathbf{u}_s\cdot\mathbf{n})}\right)_{s(u)} + \frac{1}{\gamma^2|u|} \tag{14b}$$

Note that the kernel of Eq. (14a) is explicit but the parameter u in Eq. (14b) is implicitly determined by the substitution equation. Both equations are valid for general three-dimensional trajectories. For planar trajectories the scalar products $\mathbf{u}_s\cdot\mathbf{u}_o$, $\mathbf{n}\cdot\mathbf{u}_s$ and $\mathbf{n}\cdot\mathbf{u}_o$ can be replaced by cosine functions of the angles ϕ, θ and $\phi - \theta$ that are defined in Fig. 1. To derive a simple small angle approximation all cosine functions are replaced by their second order Taylor expansion, all *factors* β are set to one and the positive part of the integration interval is neglected:

$$K(s_o, s) \approx \begin{cases} -\dfrac{\phi\theta + \gamma^{-2}}{R} - \dfrac{\theta^2/2 + 1 - \beta}{\gamma^2(s + \beta R)} & \text{for } s < 0 \\ 0 & \text{otherwise} \end{cases} \tag{15a}$$

$$\tilde{K}(s_o, u) \approx \begin{cases} -\left(\dfrac{1}{R}\cdot\dfrac{\phi\theta + \gamma^{-2}}{\theta^2/2 + 1 - \beta}\right)_{s(u)} - \dfrac{1}{\gamma^2 u} & \text{for } u < 0 \\ 0 & \text{otherwise} \end{cases} \tag{15b}$$

With $1 - \beta \approx 1/(2\gamma^2)$ Eq. (15b) is identical to the small angle approximation in [1].

An energy independent approximation can be used for $\gamma >> 1$ and bunches that are long compared to the critical wavelength ($\sigma_\lambda >> R_0/\gamma^3$):

$$4\pi\varepsilon\tilde{E} = \int \lambda'(s + R + s_0 - c_0 t)\cdot K(s_o, s)ds$$
$$K(s_o, s) = \begin{cases} \dfrac{\mathbf{n}\cdot(\mathbf{u}_s - \mathbf{u}_o) - (1 - \mathbf{u}_s\cdot\mathbf{u}_o)}{R} \approx -\dfrac{\phi\theta}{R} & \text{for } s < 0 \\ 0 & \text{otherwise} \end{cases} \tag{16}$$

It has to be mentioned that the implicit equation for the lower boundary (5) with $\beta = 1$ has not always a solution. This happens if the first part of the trajectory is a semi-infinite line and if the distance between the observer position s_o and the tail of the bunch is longer than the slippage $s_o - s_t - a$ that is defined in Fig 3. For such situations a special treatment of the integration range $s_o + s < s_t$ with $\phi = const$ and θ, R as defined in Fig. 3 is advisable. Although one can find an energy independent approximation for $\tilde{E}$ it does not always exist for the individual terms E_1 and E_2.

Some remarks about advantages and disadvantages of the formulations with $K(s_o, s)$ and $\tilde{K}(s_o, u)$. Equations with $K(s_o, s)$ can be integrated without solving an implicit equation if we abstain from the calculation of the boundaries of the integration. For some situations the integration range on a semi-infinite line before the transition to the first curvature can be quite long ($\propto \sigma_\lambda \gamma^2$). The integrals with $\tilde{K}(s_o, u)$ are convolution integrals in time. They can be solved efficiently by FFT methods if $\tilde{E}$ is required for a time interval. For trajectories that are piecewise linear both formulations can be combined: the curved parts are calculated with $K(s_o, s)$ and the linear parts with $\tilde{K}(s_o, u)$ where the implicit equation $u = s + \beta R(s)$ can be solved analytically. Both formulations of Eqs. (14) and (15) may have a numerical problem for very small values of $|s|$ or $|u|$ because the kernels are calculated as the difference of large numbers that are of the order $\gamma^{-2}|s|^{-1}$ or $\gamma^{-2}|u|^{-1}$.

2.7. Circular Motion

The longitudinal field of a bunch in circular motion has been discussed many times e.g. in [1] with approximation (15b). In the following we use approximation (15a) and estimate criterion (11) for bunches with transverse dimensions.

The distance function R and the angles ϕ, θ (compare Fig. 1) of a bunch in circular motion on a trajectory with the radius R_0 are:

$$R = \left\| \mathbf{r}_s(s_o) - \mathbf{r}_s(s_o + s) \right\| = \left| 2R_0 \sin\left(s/(2R_0)\right) \right|, \quad \phi = s/R_0\,, \quad \theta = s/\left(2R_0\right).$$

With $\gamma^2\left(s + \beta R\right) \approx \gamma^2\left(s + R\right) - R/2$ and the lowest order Taylor expansions $s + R \approx s^3/\left(24R_0^2\right)$ and $R \approx -s$ for $s < 0$ the kernel of Eq. (15a) can be written as:

$$K(s_o, s<0) \approx \frac{s}{2R_0^2}\left(1-\frac{4R_0^2\gamma^{-2}}{s^2+12R_0^2\gamma^{-2}}\right). \qquad (17)$$

The kernel and its asymptotic behavior

$$K(s_o,s) \approx \begin{cases} s/\left(3R_0^2\right) & \text{for } -R_0/\gamma << s < 0 \\ s/\left(2R_0^2\right) & \text{for } s << -R_0/\gamma \end{cases}$$

is shown in Fig. 4. The asymptotic functions are used for short- and for long-bunch-approximations.

a) The **short bunch approximation** uses the asymptotic kernel $K(s_o,s) \approx s/\left(3R_0^2\right)$ and estimates the term $s+\beta R$ in the argument of the λ' function for negative values of s by $(1-\beta)s$. The approximation is valid for bunches that are short compared to R_0/γ^3. The longitudinal field and its mean value are:

$$\tilde{E} \approx -\frac{\gamma^4}{3\pi\varepsilon R_0^2}\int_{-\infty}^{0}\lambda(u+s_o-vt)du\ , \qquad (18a)$$

$$\overline{E} = \frac{1}{q}\int\tilde{E}(t)\lambda(s_o-vt)vdt = -\frac{q\gamma^4}{6\pi\varepsilon R_0^2}\ . \qquad (18b)$$

The total energy loss $-qc\overline{E}$ is in agreement with the well known radiation power of a single particle with the charge q [7]. The transverse beam dimension $\sigma_\eta \propto \Delta_\eta$ is limited by the criterion (11) for the contributions of the split integration range. According to Eq. (10) the integration range is split into parts a and b at $-a >> \max\left(\Delta_\lambda, \Delta_\eta^2/\Delta_\lambda\right)$. To estimate the scaling of the split integrals we asume that λ' is roughly constant for $-L_\lambda < s < 0$ and zero otherwise:

$$\left|\int_{\text{part a}}\cdots ds\right| \propto \left|\int_a^0 \lambda'\cdot K(s_o,s)ds\right| \propto \left|\frac{q}{\sigma_\lambda^2}\int_a^0 K(s_o,s)ds\right| \propto a^2\ ,$$

$$\left|\int_{\text{part b}}\cdots ds\right| \propto \left|\int_{-\infty}^a \lambda'\cdot K(s_o,s)ds\right| \propto \left|\frac{q}{\sigma_\lambda^2}\int_{-L_\lambda}^a K(s_o,s)ds\right| \propto L_\lambda^2 - a^2\ ,$$

with $L_\lambda \propto \gamma^2 \sigma_\lambda$ the typical interaction length. To fulfill condition (11) the typical interaction length has to be large compared to a and therefore the transverse dimension σ_η needs to be small compared to $\gamma\sigma_\lambda$.

b) The **long bunch approximation** uses the asymptotic kernel $K(s_o, s) \approx s/\left(2R_0^2\right)$ and estimates the the term $s + \beta R$ in the argument of the λ' function for negative values of s by $s^3/\left(24R_0^2\right)$. This approximation is energy independent and valid for $\sigma_\lambda >> R_0/\gamma^3$. The substitution $u = s^3/\left(24R_0^2\right)$ is used to calculate the longitudinal field:

$$\tilde{E} \approx -\frac{1}{2\pi\sqrt[3]{3}\,\varepsilon R_0^{2/3}} \int_0^\infty \frac{\lambda(-u + s_o - vt)}{\sqrt[3]{u}} du \propto \frac{q}{\varepsilon R_0^{2/3} \sigma_\lambda^{4/3}} \ . \tag{19}$$

The longitudinal field and its mean value of a Gaussian bunch $\lambda(s) = g(s/\sigma_\lambda) q/\sigma_\lambda$ are

$$\tilde{E} \approx \frac{1}{\sqrt[3]{3}(2\pi)^{3/2}} \frac{q}{\varepsilon} \sqrt[3]{\frac{1}{R_0^2 \sigma_\lambda^4}} G\left(\frac{vt - s_o}{\sigma_\lambda}\right), \tag{20a}$$

$$\overline{E} = \frac{1}{q} \int \tilde{E}(t) \lambda(s_o - vt) v dt = -\frac{\Gamma(5/6)}{4\pi^{3/2}\sqrt[3]{6}} \frac{q}{\varepsilon R_0^{2/3} \sigma_\lambda^{4/3}}, \tag{20b}$$

with $g(s)$ the gaussian normal distribution and the shape function

$$G(x) = \sqrt{2\pi} \int_0^\infty \frac{g'(x + \xi)}{\sqrt[3]{\xi}} d\xi$$

that is plotted in Fig. 5. The limitation for the transverse beam dimension σ_η can be estimated in almost the same manner as for short bunches with the exception that the typical interaction length is $L_\lambda = \sqrt[3]{24 R_0^2 \sigma_\lambda}$. Therefore the transverse beam dimension has to be small compared to $\sqrt{L_\lambda \sigma_\lambda} \propto \sqrt[3]{R_0 \sigma_\lambda^2}$.

2.8. Example 1, Part 1: Circular Motion, Energy Dependent Approximation

The complete longitudinal field $E = \tilde{E} + E_l$ is calculated for a spherical Gaussian bunch on a circular trajectory with the radius $R_0 = 10\,\text{m}$. The bunch charge and

dimensions are $q = 1\,\mathrm{nC}$ and $\sigma_\lambda = \sigma_\eta = 100\mu\mathrm{m}$. Eq. (14a) is used for $\tilde{E}$ and the linear motion contribution E_l is computed by

$$4\pi\varepsilon E_l = \frac{-q}{\gamma\sigma_\lambda\sigma_\eta}\int g'(x + (s_o - vt)/\sigma_\lambda)F(x\gamma\sigma_\lambda/\sigma_\eta)dx \ , \qquad (21)$$

with

$$F(x) = \sqrt{\frac{\pi}{2}}\exp\left(\frac{\xi^2}{2}\right)\left(1 - \mathrm{erf}\left(\frac{|\xi|}{\sqrt{2}}\right)\right) \approx \frac{1}{\sqrt{1+\xi^2}} \quad \text{for } |\xi| >> 1 \ .$$

This equation is valid for Gaussian bunches with arbitrary aspect ration $\sigma_\eta/\sigma_\lambda$. The field for γ=50, 100, 200 and 1000 is shown in Fig. 6. It can be seen that the curve for the lowest energy is dominated by the 'linear motion' contribution $\propto \gamma^{-2}\lambda'$ and that the curves approach the energy independent shape (compare Fig. 5) with increasing value of γ. As E_l is antisymmetric it does not contribute to the total energy loss $P = -\beta c^2 \int E(t)\lambda(-vt)dt$. The total energy losses are 34.76 kW, 43.00 kW, 43.77 kW, 43.83 kW and 43.83 kW for γ=50, 100, 200, 1000 and for the energy independent approximation $-qc\overline{E}$ with Eq. (20b).

2.9. Example 2: Helical Motion, Energy Independent Approximation

The helical trajectory is a simple example of none-planar motion. The path function and the tangential vector of the helix are

$$\mathbf{r}_s(s) = R_d\cos(s/R_r)\mathbf{u}_x + R_d\sin(s/R_r)\mathbf{u}_y + s\sqrt{1 - R_d^2/R_r^2}\,\mathbf{u}_z \,,$$

$$\mathbf{u}_s(s) = -R_d/R_r\sin(s/R_r)\mathbf{u}_x + R_d/R_r\cos(s/R_r)\mathbf{u}_y + \sqrt{1 - R_d^2/R_r^2}\,\mathbf{u}_z \ ,$$

with R_d the diameter, $2\pi R_r$ the revolution length and $h = 2\pi\sqrt{R_r^{\,2} - R_d^2}$ the height of one winding. It can be verified that the term $\mathbf{n}\cdot(\mathbf{u}_s - \mathbf{u}_o)$ is zero as it was mentioned above. For the argument of λ' we use the lowest order Taylor expansion of

$$s + \beta R = s + \beta\left\|\mathbf{r}_s(s_o) - \mathbf{r}_s(s_o + s)\right\| \approx \frac{\mathrm{s}^3}{24\left(R_r^2/R_d\right)^2}$$

with $\beta \to 1$ and for $s < 0$. The term $1 - \mathbf{u}_s \cdot \mathbf{u}_o = (R_d / R_r)^2 \left(1 - \cos(s/R_r)\right)$ in Eq. (16) is also replaced by its lowest order Taylor expansion so that we get the energy independent kernel:

$$K(s_o, s < 0) = -\frac{(1 - \mathbf{u}_s \cdot \mathbf{u}_o)}{R} \approx \frac{s}{2\left(R_r^2 / R_d\right)^2} \ .$$

The expressions for the argument of λ' and for the kernel are formally identical to that of circular motion if one replaces R_r^2 / R_d by R_0. Therefore the longitudinal field $\tilde{E}$ follows by analogy to Eq. (20) as

$$\tilde{E} \approx \frac{1}{\sqrt[3]{3}(2\pi)^{3/2}} \frac{q}{\varepsilon} \sqrt[3]{\frac{R_d^2}{R_r^4 \sigma_\lambda^4}} G\left(\frac{vt - s_o}{\sigma_\lambda}\right) .$$

The term R_r^2 / R_d is identical to the curvature radius $\left\|\mathbf{u}_s'\right\|^{-1}$. Note that this approach is not appropriate to calculate the radiation of micro-bunches in a helical undulator because criterion (11) is not fulfilled for typical aspect ratios $\sigma_\eta / \sigma_\lambda$ in FELs.

2.10. Example 3, Part 1: Bunch-Compressor

The trajectory in dispersive bunch-compressors with several bending magnets can be described by a sequence of arcs and lines. In such devices long range interactions can take place that involve several elements (e.g. arc-line-arc or line-arc-line[10]). This is shown for the benchmark example of the bunch compressor of the CSR workshop in Zeuthen 2002 [11]. The example consists of a simple four-bend chicane with parameters similar to those required for the compression stages of the LCLS (at 5 GeV) or TESLA XFEL (at 500 MeV). All four magnets have the same length (0.5 m) and bending radius (10 m). The length of the drifts between the first and last two magnets is 5 m and the middle magnets are separated by a 1 m drift. We calculate the longitudinal electric field $E = \tilde{E} + E_l$ for a 1 nC bunch with $\sigma_\eta = 100\mu$m and $\gamma = 1000$ for several positions in the chicane. The fixed bunch length of $\sigma_\lambda = 20\mu$m corresponds to the beam dimension after compression. We did not change the bunch length (as it happens during compression) to allow the comparison of fields at the same relative position with respect to different magnets. Fig. 7 shows the time-dependent field for a position 15 cm after the beginning of the magnets. The field is

similar (but not exactly identical) in magnet 1, 2 and 4 but obviously different in the third magnet that is separated by a shorter drift (of 1 m) from the previous bending magnet. Therefore the CSR radiation from the second magnet is not quite negligible at this position. Even after a longer drift (of 5 m) the CSR radiation of earlier magnets contributes to the field as it can be seen in Fig. 8 for a position 45 cm after the magnet entrance. The late part of the signal (for $vt - s_o > -3\sigma_\lambda$) has approached the steady state solution that is given by Eqs. (20a, 21). The early peak in the first magnet ($vt - s_o \approx -6.2\,\sigma_\lambda$) is the wave-front that was in the plane perpendicular to the bunch *before* the charge had entered the magnet. At this location the information that the bunch is no longer in linear motion has not reached the observer and therefore the 'old' front is seen. In principle the same effect is active in Fig. 7 but there the angle between the particle motion and the wave propagation is smaller as well as the slippage between the bunch and the wave, so that it is not possible to distinguish the 'old' wave-front from radiative fields that have been created *in* the magnet. The other early fronts in Fig. 8 (at $vt - s_o \approx -7.2\,\sigma_\lambda$ for magnets 2 and 4, at $vt - s_o \approx -7.6\,\sigma_\lambda$ for magnet 3) are related to radiation from the previous magnets. In Fig. 9 for a positions 10 cm after the magnet, these fronts are earlier (or further ahead of the bunch) and in Fig. 10 they are outside the picture. The later part of the signal is identical for all magnets and independent of the history before the magnets. Note that it *seems* that the wave-fronts are faster than a bunch that is in linear motion with nearly the velocity of light.

The projected longitudinal and transverse dimensions of a bunch (with energy chirp) at the end of the third magnet are $\sigma_\lambda = 20\,\mu\text{m}$ and $\sigma_\eta = 2\,\text{mm}$. Therefore the (projected) transverse beam dimension is not small compared to $\sqrt[3]{R_0\sigma_\lambda^2} = 1.6\,\text{mm}$ as is required for the applicability of the one-dimensional theory.

In appendix 1 the complete MATHCAD program [9] is listed that was used to calculate the curves in Figs. 7, 8, 9 and 10. The program is neither optimized for accuracy nor for efficiency. The only measure that is used to ensure the convergence of the numerical integration is the splitting of the full integrals into integrals over subintervals.

3. Complete Field of Spherical Gaussian Bunches

The electromagnetic fields as well as the scalar and vector potentials of a rigid spherical gaussian bunch in general translatory motion can be calculated without any approximations by a one dimensional integration for any observer position.

3.1. Scalar and Vector Potential

The source distributions $\rho(\mathbf{r},t)$ and $\mathbf{J}(\mathbf{r},t)$ of a spherical gaussian bunch are defined by

$$\rho(\mathbf{r},t) = \rho_s(\mathbf{r} - \mathbf{r}_t(t)) \,, \tag{22a}$$

$$\mathbf{J}(\mathbf{r},t) = \rho_s(\mathbf{r} - \mathbf{r}_t(t))\mathbf{v}_t(t) \,, \tag{22b}$$

$$\rho_s(\mathbf{r}) = \frac{q}{(2\pi)^{3/2}\sigma^3}\exp\left(-\frac{1}{2}\frac{\|\mathbf{r}\|^2}{\sigma^2}\right) , \tag{22c}$$

with $\rho_s(\mathbf{r})$ the shape function, σ the rms radius of the bunch, $\mathbf{r}_t(t)$ the time dependent path function and $\mathbf{v}_t(t) = \dot{\mathbf{r}}_t(t)$ the velocity. The three dimensional integral for the scalar potential is modified by a shift of the integration parameter $\mathbf{r}'$ so that the observer is at the origin of the new coordinate system:

$$\Phi(\mathbf{r},t) = \frac{1}{4\pi\varepsilon}\int\frac{\rho(\mathbf{r}',t')}{\|\mathbf{r}-\mathbf{r}'\|}dV' = \frac{1}{4\pi\varepsilon}\int\frac{\rho_s(\mathbf{r}'+\mathbf{r}-\mathbf{r}_t(t'))}{\|\mathbf{r}'\|}dV' .$$

Therefore the three-dimensional volume integration can be considered as a sequence of a two-dimensional integrations over the surface of a sphere with radius r' around the observer and a one-dimensional integration along the radial coordinate. As the retarded time $t' = t - r'/c$ is the same for all points on the spherical surface (with fixed radius) the two-dimensional integral can be solved analytically. The scalar potential can be computed by the one-dimensional integration

$$\Phi(\mathbf{r},t) = \frac{q}{\varepsilon(2\pi)^{3/2}\sigma^2}\int_0^\infty f\left(\frac{r'}{\sigma},\frac{R(r',\mathbf{r},t)}{\sigma}\right)dr' \,, \tag{23a}$$

with the auxiliary function

$$f(a,b) = \exp\left(-\frac{a^2+b^2}{2}\right)\frac{\sinh(ab)}{b} = \sqrt{\frac{\pi}{2}}\frac{1}{b}\left(g(a-b)-g(a+b)\right) \tag{23b}$$

and the distance function $R(r',\mathbf{r},t) = \left\|\mathbf{r} - \mathbf{r}_t\left(t - r'/c\right)\right\|$ to the retarded origin of the observer. The calculation of the vector potential is equivalent:

$$\mathbf{A}(\mathbf{r},t) = \frac{q\mu}{(2\pi)^{3/2}\sigma^2}\int_0^\infty \mathbf{v}(t-r'/c)\; f\left(\frac{r'}{\sigma},\frac{R(r',\mathbf{r},t)}{\sigma}\right)dr' . \tag{24}$$

As in the last section we suppress the arguments of some functions in one-dimensional integrals and use the following notation:

$$R = R(r',\mathbf{r},t) = \left\|\mathbf{r} - \mathbf{r}_t\left(t - r'/c\right)\right\|$$
$$\mathbf{n} = \mathbf{n}(r',\mathbf{r},t) = \frac{\mathbf{r} - \mathbf{r}_t(t-r'/c)}{\left\|\mathbf{r} - \mathbf{r}_t(t-r'/c)\right\|}$$
$$\mathbf{v} = \mathbf{v}(t-r'/c)\,,\quad \boldsymbol{\beta} = c^{-1}\mathbf{v}(t-r'/c)$$
$$\dot{\mathbf{v}} = \dot{\mathbf{v}}(t-r'/c)\,,\quad \dot{\boldsymbol{\beta}} = c^{-1}\dot{\mathbf{v}}(t-r'/c)$$

3.2. Derivatives of Potentials

The temporal and spatial derivatives of the potentials are needed for the calculation of electromagnetic field quantities. They follow directly from Eqs. (23, 24), using the formal rules for derivations, as:

$$\partial_t \Phi(\mathbf{r},t) = \frac{-q}{\varepsilon(2\pi)^{3/2}\sigma^3}\int_0^\infty \mathbf{n}\cdot\mathbf{v}\; \tilde{f}\left(\frac{r'}{\sigma},\frac{R(r',\mathbf{r},t)}{\sigma}\right)dr' \;, \tag{25a}$$

$$\partial_t \mathbf{A}(\mathbf{r},t) = \frac{q\mu}{(2\pi)^{3/2}\sigma^3}\left(\sigma\int_0^\infty \dot{\mathbf{v}}\; f(\cdots)dr' - \int_0^\infty (\mathbf{n}\cdot\mathbf{v})\mathbf{v}\; \tilde{f}(\cdots)dr'\right) , \tag{25b}$$

$$\nabla\Phi(\mathbf{r},t) = \frac{q}{\varepsilon(2\pi)^{3/2}\sigma^3}\int_0^\infty \mathbf{n}\; \tilde{f}\left(\frac{r'}{\sigma},\frac{R(r',\mathbf{r},t)}{\sigma}\right)dr' \;, \tag{25c}$$

$$\nabla\times\mathbf{A}(\mathbf{r},t) = \frac{q\mu}{(2\pi)^{3/2}\sigma^3}\int_0^\infty \mathbf{n}\times\mathbf{v}\; \tilde{f}\left(\frac{r'}{\sigma},\frac{R(r',\mathbf{r},t)}{\sigma}\right)dr' \;, \tag{25d}$$

with

$$\mathbf{n} = \mathbf{n}(r',\mathbf{r},t) = \frac{\mathbf{r} - \mathbf{r}_t(t-r'/c)}{\left\|\mathbf{r} - \mathbf{r}_t(t-r'/c)\right\|}, \tag{25d}$$

$$\tilde{f}(a,b) = \exp\left(-\frac{a^2+b^2}{2}\right)\left(\frac{a}{b}\cosh(ab) - \left(1+\frac{1}{b^2}\right)\sinh(ab)\right) . \qquad (25e)$$

We used $\partial_b f(a,b) = \tilde{f}(a,b)$, $\partial_t R(r',\mathbf{r},t) = -\mathbf{n}\cdot\mathbf{v}$ and $\partial_{r'} R(r',\mathbf{r},t) = \mathbf{n}\cdot\boldsymbol{\beta}$.

3.3. Electromagnetic Fields

The one-dimensional integrals for the electric field $\mathbf{E} = -\nabla\phi - \partial_t \mathbf{A}$ and the magentic flux density $\mathbf{B} = \nabla\times\mathbf{A}$ are:

$$\mathbf{E}(\mathbf{r},t) = \frac{q}{\varepsilon(2\pi)^{3/2}\sigma^3}\left(\int_0^\infty ((\mathbf{n}\cdot\boldsymbol{\beta})\boldsymbol{\beta} - \mathbf{n})\,\tilde{f}(\cdots)dr' - \frac{\sigma}{c^2}\int_0^\infty \dot{\mathbf{v}}\, f(\cdots)dr'\right) , \qquad (26a)$$

$$\mathbf{B}(\mathbf{r},t) = \frac{q\mu}{(2\pi)^{3/2}\sigma^3}\int_0^\infty \mathbf{n}\times\mathbf{v}\,\tilde{f}\left(\frac{r'}{\sigma}, \frac{R(r',\mathbf{r},t)}{\sigma}\right)dr' . \qquad (26b)$$

3.4. Outlying Observer and Liénard Wiechert Potentials

The integration range of Eqs. (23, 24, 26) can be reduced to a finite interval if we neglect contributions of the Gaussian functions in Eq. (23b) for arguments $|a-b| > x >> 1$ or $|r' - R(r',\mathbf{r},t)| > \Delta$ with $\Delta = x\sigma$. The upper boundary r'_u is the solution of the implicit equation $r'_u - R(r'_u,\mathbf{r},t) = \Delta$. The lower boundary r'_l has a positive solution of $R(r',\mathbf{r},t) - r' = \Delta$ for observers that are outside the truncated source distribution. In this context we call an observer 'outlying' if the term $\propto g(a+b)$ in Eq. (23b) is negligible for the *complete* integration range $[r'_l, r'_u]$. This is fulfilled if $r'_l > \Delta$ or if the observer is outside a sphere with radius 2Δ around $\mathbf{r}_t(t-\Delta/c)$. For outlying observers the auxiliary function and its derivative can be replaced by

$$f(a,b) = \sqrt{\frac{\pi}{2}}\frac{1}{b}g(a-b) , \qquad (27a)$$

$$\tilde{f}(a,b) = -\sqrt{\frac{\pi}{2}}\frac{1}{b}g'(a-b) - \sqrt{\frac{\pi}{2}}\frac{1}{b^2}g(a-b) . \qquad (27b)$$

With the Gaussian function $g^{(\sigma)}(x) = g(x/\sigma)/\sigma$ and its derivative $g'^{(\sigma)}(x)$ the scalar and vector potentials follow as

$$\Phi(\mathbf{r},t)=\frac{q}{4\pi\varepsilon}\int_{r'_l}^{r'_u}\frac{g^{(\sigma)}(r'-R(r',\mathbf{r},t))}{R(r',\mathbf{r},t)}dr' \ , \tag{28a}$$

$$\mathbf{A}(\mathbf{r},t)=\frac{q\mu}{4\pi}\int_{r'_l}^{r'_u}\mathbf{v}\frac{g^{(\sigma)}(r'-R(r',\mathbf{r},t))}{R(r',\mathbf{r},t)}dr' \ . \tag{28b}$$

For point particles ($\sigma \to 0$) the gaussian function $g^{(\sigma)}(x)$ can be substituted by the dirac function $\delta(x)$ that can be integrated by use of the property

$$\int Q(\cdots)\delta(r'-R(r',\mathbf{r},t))dr'=\left(\frac{Q(\cdots)}{\partial_{r'}(r'-R(r',\mathbf{r},t))}\right)_{r'}=\left(\frac{Q(\cdots)}{1-\mathbf{n}\cdot\boldsymbol{\beta}}\right)_{r'}$$

with r' the solution of the implicit equation $r'=R(r',\mathbf{r},t)$. This leads to the well known Liénard-Wiechert potentials:

$$\Phi(\mathbf{r},t)=\frac{q}{4\pi\varepsilon}\left(\frac{1}{r'(1-\mathbf{n}\cdot\boldsymbol{\beta})}\right)_{r'} \ , \tag{29a}$$

$$\mathbf{A}(\mathbf{r},t)=\frac{q\mu}{4\pi}\left(\frac{\mathbf{v}}{r'(1-\mathbf{n}\cdot\boldsymbol{\beta})}\right)_{r'} \ . \tag{29b}$$

The calculation of the Liénard-Wiechert field equations from Eqs. (26, 27) with $\sigma \to 0$ is similar. This is shown in appendix 2 for the electric field of a point particle.

3.5. Example 3, Part 2: Bunch-Compressor

Eqs. (26a, b) have been used to calculate the electromagnetic field in the center of a spherical bunch that travels through the four magnet chicane which has been described earlier. The charge of the bunch is 1 nC, the rms radius is $\sigma = 20\,\mu$m and its Lorentz factor is $\gamma = 1000$. In Fig. 11 the longitudinal field is shown as a function of the position in the bunch-compressor. (The $\hat{s}$-range of the first magnet is 0…0.5 m, the second magnet is between 5.5 m and 6m, the third and fourth magnet are in the intervals 7…7.5 m and 12.5…13 m.) The longitudinal field reaches its steady state value for circular motion approximately at the end of the magnets. The integrated contributions from the drifts is certainly not negligible compared to that of the arcs. Both methods Eq. (26a) and Eq. (14a) are in good agreement. The transverse

component of the Lorentz force $F_\perp$ and the transverse magnetic field can be seen in Figs. 12 and 13. Fig. 14 shows a magnified view of $F_\perp$ in the range of magnets two and three together with the product of Φ, the scalar potential and K, the inverse curvature radius. The change of potential energy $\propto \Delta\Phi$ contributes to the change of the total particle energy $\Delta\mathcal{E}$. Both terms $F_\perp$ and $K\Delta\mathcal{E}$ appear on the right hand side of the transverse equation of motion, but the different transient behaviour of $F_\perp$ and $K\Phi$ clearly demonstrates that no effective cancellation can be used for the integration of the transverse equation of motion [12].

3.6. Generalization and Planar Approximation

To organize the three-dimensional retarded source integration for an arbitrary distribution $\rho(\mathbf{r},t)=\rho_s(\mathbf{r}-\mathbf{r}_t(t))$ with fixed shape, we redefine the auxiliary functions:

$$f(r',\mathbf{w})=\frac{1}{r'}\int_{K(r')}\rho_s(\mathbf{r}'+\mathbf{w})dA' \ , \tag{30a}$$

$$\tilde{\mathbf{f}}(r',\mathbf{w})=\nabla_w f(r',\mathbf{w}) \ , \tag{30b}$$

with $K(r')$ the surface of a sphere with radius r' around the origin. Therefore the scalar- and vector-potential are r'-integrals of the auxiliary function f:

$$\Phi(\mathbf{r},t)=\frac{1}{4\pi\varepsilon}\int\frac{\rho(\mathbf{r}',t')}{\|\mathbf{r}-\mathbf{r}'\|}dV'=\frac{q}{4\pi\varepsilon}\int_0^\infty f(r',\mathbf{r}-\mathbf{r}_t(t'))dr' \ , \tag{31a}$$

$$\mathbf{A}(\mathbf{r},t)=\frac{q\mu}{4\pi}\int_0^\infty \mathbf{v}\ f(r',\mathbf{r}-\mathbf{r}_t(t'))dr' \ . \tag{31b}$$

The electromagnetic fields are integrals of the auxiliary function f and its gradient $\tilde{\mathbf{f}}$:

$$\mathbf{E}(\mathbf{r},t)=\frac{q}{4\pi\varepsilon}\int_0^\infty\left\{(\boldsymbol{\beta}\otimes\boldsymbol{\beta}-\mathbf{I})\tilde{\mathbf{f}}(r',\mathbf{r}-\mathbf{r}_t(t'))-\frac{\dot{\boldsymbol{\beta}}}{c}\ f(r',\mathbf{r}-\mathbf{r}_t(t'))\right\}dr' \ , \tag{32a}$$

$$\mathbf{B}(\mathbf{r},t)=\frac{q\mu}{4\pi}\int_0^\infty\tilde{\mathbf{f}}(r',\mathbf{r}-\mathbf{r}_t(t'))\times\mathbf{v}dr' \ . \tag{32b}$$

For values of r' that are large compared to the dimensions of ρ_s the spherical integration for the auxiliary function can be replaced by a planar integration as sketched in Fig. 15:

$$f(r',\mathbf{w}) = \frac{1}{r'} \int\limits_{\mathbf{r}\cdot\mathbf{k}=1} \rho_s(\mathbf{r}) dA' \text{ with } \mathbf{k}(r',\mathbf{w}) = \mathbf{w} - r' \frac{\mathbf{w}}{\|\mathbf{w}\|} . \tag{33}$$

This integration can be solved analytically for general Gaussian bunches

$$\rho_s(\mathbf{r}) = \frac{q\sqrt{\det \mathbf{M}}}{(2\pi)^{3/2}} \exp\left(-\frac{1}{2} \mathbf{r}^t \mathbf{M} \mathbf{r} \right) , \tag{34}$$

with $\mathbf{M}$ symmetric and positive definite. The planar approximations of the auxiliary functions of Gaussian distributions are:

$$f_p(r',\mathbf{w}) = \frac{q}{r'} g^{(\sigma_w)}(\|\mathbf{w}\| - r') , \tag{35a}$$

$$\tilde{\mathbf{f}}_p(r',\mathbf{w}) = \frac{q}{r'} \left\{ g'^{(\sigma_w)}(w - r') \frac{\mathbf{w}}{w} + g''^{(\sigma_w)}(\|w\| - r') \frac{1}{w^2} \left(\mathbf{M}^{-1} \frac{\mathbf{w}}{w} - \sigma_w^2 \frac{\mathbf{w}}{w} \right) \right\}, \tag{35b}$$

with the projected bunch length

$$\sigma_w = \frac{\sqrt{\mathbf{w}^t \mathbf{M}^{-1} \mathbf{w}}}{\|\mathbf{w}\|} .$$

The disadvantage of the planar approximation is that it can be used only for a part of the integration range or for observers that are sufficiently far away from the source e.g. for observers that are ahead. To avoid this, an extraction technique is proposed that is similar to the extraction of the 'linear motion' part in the first method.

3.7. Extraction Approximation

The extraction approach uses an estimation of the near contributions to the integrals for $\mathbf{E}$ and $\mathbf{B}$:

$$\mathbf{N}_E(f, \tilde{\mathbf{f}}) \approx (\boldsymbol{\beta} \otimes \boldsymbol{\beta} - \mathbf{I}) \tilde{\mathbf{f}}(r', \mathbf{r} - \mathbf{r}_t(t')) - \frac{\dot{\boldsymbol{\beta}}}{c} f(r', \mathbf{r} - \mathbf{r}_t(t')) , \tag{36a}$$

$$\mathbf{N}_B(f, \tilde{\mathbf{f}}) \approx \tilde{\mathbf{f}}(r', \mathbf{r} - \mathbf{r}_t(t')) \times \mathbf{v} . \tag{36b}$$

These contributions are extracted and incomplete fields $\mathbf{E}_i$ and $\mathbf{B}_i$ are integrated. To complete the total fields, the extracted parts $\mathbf{E}_e$ and $\mathbf{B}_e$ are integrated seperately and added. To approximate the incomplete fields they are integrated with the planar approximation of the auxilliary function. The approach is based on the assumption that the systematic errors in the modified original terms and the modified extracted parts are similar and cancel sufficiently. Of course the extracted parts $\mathbf{E}_e$ and $\mathbf{B}_e$ have to be calculated with the exact auxiliary functions. This proceedure is numerically efficient if the effort for the calculation of the extracted parts is small compared to a direct integration of Eq. (32).

To use this technique the near contributions to the integrals in Eq. (32) have to be estimated. Therefore we approximate the position and velocity of the bunch center by a first order expansion:

$$\mathbf{r}_l(t') = \mathbf{r}_{l0} + c(t'-t)\boldsymbol{\beta}_{l0} = \mathbf{r}_{l0} - r'\boldsymbol{\beta}_{l0} \ ,$$

$$\boldsymbol{\beta}_l(t') = \boldsymbol{\beta}_{l0} + (t'-t)\dot{\boldsymbol{\beta}}_{l0} = \boldsymbol{\beta}_{l0} - r'\dot{\boldsymbol{\beta}}_{l0} \ ,$$

and the acceleration by $\dot{\boldsymbol{\beta}}_l(t) = \dot{\boldsymbol{\beta}}_{l0}$, with $\mathbf{r}_{l0} = \mathbf{r}_t(t)$, $\boldsymbol{\beta}_{l0} = \boldsymbol{\beta}(t)$ and $\dot{\boldsymbol{\beta}}_{l0} = \dot{\boldsymbol{\beta}}(t)$ the instantaneous position, velocity and acceleration. We replace the corresponding path functions in Eq. (36) and neglect quadratic terms in r':

$$\mathbf{N}_E\left(f, \tilde{\mathbf{f}}\right) = \left(\mathbf{T}_0 - \frac{r'}{c}\mathbf{T}_1\right)\tilde{\mathbf{f}}\left(r', \mathbf{r} - \mathbf{r}_l(t')\right) - \frac{\dot{\boldsymbol{\beta}}_{l0}}{c} f\left(r', \mathbf{r} - \mathbf{r}_l(t')\right) \ , \tag{37a}$$

$$\mathbf{N}_B\left(f, \tilde{\mathbf{f}}\right) = c\tilde{\mathbf{f}}\left(r', \mathbf{r} - \mathbf{r}_l(t')\right) \times \boldsymbol{\beta}_l \ , \tag{37b}$$

with the constant tensors $\mathbf{T}_0 = \boldsymbol{\beta}_{l0} \otimes \boldsymbol{\beta}_{l0} - \mathbf{I}$ and $\mathbf{T}_1 = \boldsymbol{\beta}_{l0} \otimes \dot{\boldsymbol{\beta}}_{l0} + \dot{\boldsymbol{\beta}}_{l0} \otimes \boldsymbol{\beta}_{l0}$. Therefore the incomplete fields are approximated by:

$$\mathbf{E}_i = \frac{q}{4\pi\varepsilon} \int_0^\infty \left\{ (\boldsymbol{\beta} \otimes \boldsymbol{\beta} - \mathbf{I})\tilde{\mathbf{f}}_p - \frac{\dot{\boldsymbol{\beta}}}{c} f_p - \mathbf{N}_E\left(f_p, \tilde{\mathbf{f}}_p\right) \right\} dr' \ , \tag{38a}$$

$$\mathbf{B}_i = \frac{q\mu}{4\pi} \int_0^\infty \left\{ \tilde{\mathbf{f}}_p \times \mathbf{v} - \mathbf{N}_B(f_p, \tilde{\mathbf{f}}_p) \right\} dr' \ , \tag{38b}$$

and the extracted parts are

$$\mathbf{E}_e = \frac{q}{4\pi\varepsilon}\int_0^\infty \mathbf{N}_E\left(f, \tilde{\mathbf{f}}\right)dr' = \mathbf{T}_0\nabla\Phi_l - c^{-1}\mathbf{T}_1\nabla_{\boldsymbol{\beta}_l}\Phi_l - c^{-1}\dot{\boldsymbol{\beta}}_{l0}\Phi_l \ , \qquad (39a)$$

$$\mathbf{B}_e = \frac{q\mu}{4\pi}\int_0^\infty \mathbf{N}_B(f_p, \tilde{\mathbf{f}}_p)dr' = c^{-1}\nabla\Phi_l \times \boldsymbol{\beta}_{l0} - c^{-2}\nabla_{\boldsymbol{\beta}_l}\Phi_l \times \dot{\boldsymbol{\beta}}_{l0} \ , \qquad (39b)$$

with Φ_l the scalar potential of the distribution in linear motion, $\nabla\Phi_l$ the gradient of the linear motion scalar potential and

$$\nabla_{\boldsymbol{\beta}_l}\Phi_l(\mathbf{r}, t) = \frac{q}{4\pi\varepsilon}\int_0^\infty \tilde{\mathbf{f}}(r', \mathbf{r} - \mathbf{r}_l(t'))r'dr' \ .$$

One crucial point of the extraction approximation is to find a way to calculate Φ_l, $\nabla\Phi_l$ and $\nabla_{\boldsymbol{\beta}_l}\Phi_l$ with similar or less effort than is required for Eq. (38). As these quantities are related to a Poisson problem they can be evaluated very efficiently on a grid. Therefore the advantages of Poisson solvers can be utilized if the field quantities are not only required for one but for a set of observation points on a mesh.

3.8. Example 1, Part 2: Circular Motion

The extraction approximation is tested for a flat elliptical bunch in circular motion with the parameters, dimensions and the orientation as shown in Fig. 16. The example demonstrates that the extraction approximation is applicable for extreme problems using a large aspect ratio of the rms dimensions and a projected length that differs considerably from the local bunch length as well as from the projected transverse dimensions. The scenario in Fig. 16 for orientation (a) is an improved description of the compression process in the third magnet of a four-magnet bunch-compressor chicane. The projected bunch length at the observation point is $20\,\mu\mathrm{m}$. At an observation point that is one typical interaction length ($\sqrt[3]{34R_0^2\sigma} \approx 36\,\mathrm{cm}$) upstream, the projected bunch length is $38\,\mu\mathrm{m}$. It is obvious that the dynamic variation of the length of the retarded bunch is not negligible. In Figs. 17 and 18 the longitudinal field and the transverse component of the Lorentz force along one of the main axes of the ellipsoid are shown. The agreement with the longitudinal field calculated by an exact three-dimensional integration and the planar approach is good, but the one-dimensional approximation (Eq. (20)) differs by approximately $0.5\,\mathrm{MV/m}$ in the core of the distribution. Orientation (b) in Fig. 16 corresponds to a situation after

overcompression. At an observation point that is $39\,\mathrm{cm}$ upstream, the long main axis of the distribution is perpendicular to the trajectory so that the projected bunch length is given by the dimension of the short main axis of $5\,\mu\mathrm{m}$. During one typical interaction length the projected length of the retarded distribution is increased by almost a factor of four! The longitudinal field differs substantially from that of orientation (a) and of the one-dimensional calculation. The complete curve is shifted to more positive values and tail particles that are more that 1.7σ behind gain energy. The planar approximation describes the qualitative behaviour correctly, but the agreement to the exact curve is not really impressive. These differences are not caused by an insufficient compensation of near terms in the field integrals, but by errors of the planar approximation for r' in the range of $20\,\mathrm{cm}$ to $40\,\mathrm{cm}$. On one side this range contributes essentially to the total integral, but on the other side the surface of the spherical integration is nearly perpendicular to the short main axis of the retarded distribution. As the distribution is wide in the plane used by the planar approximation (compare Fig. 15) but 100 times shorter in the perpendicular direction, the curvature of the spherical integration surface is not quite negligible. Therefore the planar approximation is not too precise for this situation. The accuracy can be improved by the use of several sub-bunches with smaller dimensions.

4. Conclusion/Summary

Two methods have been presented to calculate the longitudinal field of a bunch with arbitrary longitudinal shape for observers that are on the trajectory and to calculate all electromagnetic field quantities of spherical Gaussian bunches at arbitrary observer positions. Both methods can be used for general trajectories, e.g. for the sequence of arcs and drifts in bunch-compressors. Their effort is determined by a one-dimensional integration. The restriction for the first method (“longitudinal field on the trajectory”) to the ratio of longitudinal to transverse beam dimensions is not always fulfilled in real bunch-compressors. The method for spherical Gaussian bunches is valid without limitation. An approach for arbitrary Gaussian distributions is proposed that is also numerically efficient if the required correction terms can be calculated simultaneously for several observer positions by a Poisson integration technique.

5. Acknowledgement

The author sincerely thanks E. Saldin, E. Schneidmiller, M. Yurkov, T. Limberg, Y. Kim, K. Flöttmann, Ph. Piot, J. Rossbach, F. Stulle, B. Beutner, V. and J. Maksimovic, U. v. Rienen and S. Wipf for many useful discussions and comments on this work.

References

[1] E. Saldin, E. Schneidmiller, M. Yurkov: Radiative Interaction of Electrons in a Bunch Moving in an Undulator. NIM A417 (1998) 158-168.

[2] M. Borland: Simple method for particle tracking with coherent synchrotron radiation. Phys. Rev. Special Topics – Accelerators and Beams, Vol. 4, 070701 (2001).

[3] M. Dohlus, T. Limberg: Emittance Growth due to Wake Fields on Curved Bunch Trajectories. International FEL Conference (Rome, 1996), TESLA-FEL 96-13. 1995.

[4] R. Li, Self-Consistent Simulation of the CSR Effect. NIM A429 (1998) 310-314.

[5] L. Gianessi, M. Quattromini: TREDI: A Self Consistent Three-Dimensional Integration Scheme for RF-Gun Dynamics Based on the Liénard-Wiechert Potentials Formalism. In Proceedings of the workshop towards X-ray free electron lasers, Gargano, Italy 1997. AIP Conf. Proceedings 413, (1997) 313.

[6] M. Dohlus, A. Kabel, T. Limberg: Efficient Field Calculation of 3D Bunches on General Trajectories. NIM A445 (2000) 338-342.

[7] J. Jackson: Classical Electrodynamics. (John Wiley and Sons, New York, 1975).

[8] Y. Derbenev, J. Rossbach, E. Saldin, V. Shiltsev: Microbunching Radiative Tail-Head Interaction. TESLA-FEL 95-05, September 95.).

[9] MathSoft, Inc.: http://www.mathsoft.com, MATHCAD 2001 Professional.

[10] E. Saldin, E. Schneidmiller, M. Yurkov: On the Coherent Radiation of an Electron Bunch Moving in an Arc of a Circle. NIM A398 (1997) 373-394.

[11] CSR Workshop, Zeuthen Jan. 2002, http://www.desy.de/csr/csr_workshop_2002/csr_workshop_2002_index.html.

[12] G. Geloni, E. Saldin, E. Schneidmiller, M. Yurkov: Misconceptions Regarding the Cancellation of Self-Forces in the Transverse Equation of Motion for an Electron in a bunch. DESY-03-165.

Appendix 1: MATHCAD Program for Bunch-Compressor Example

1. Physical Parameters

$c_0 := 2.998 \cdot 10^{8} \quad \mu_0 := 4 \cdot \pi \cdot 10^{-7} \quad \varepsilon_0 := \frac{1}{c_0^{\,2} \cdot \mu_0}$

2. Bunch and Energy

$\sigma_\lambda := 20 \cdot 10^{-6} \quad \sigma_\eta := 100 \cdot 10^{-6} \quad q_0 := 10^{-9}$

$\gamma := 1000 \quad \beta := \sqrt{1 - \gamma^{-2}} \quad v := \beta \cdot c_0$

$$\lambda(s) := \frac{q_0}{\sqrt{2 \cdot \pi} \cdot \sigma_\lambda} \cdot \exp\left[\frac{-1}{2} \cdot \left(\frac{s}{\sigma_\lambda}\right)^2\right] \quad \lambda s(s) := \frac{-q_0 \cdot s}{\sqrt{2 \cdot \pi} \cdot \sigma_\lambda^{\,3}} \cdot \exp\left[\frac{-1}{2} \cdot \left(\frac{s}{\sigma_\lambda}\right)^2\right]$$

3. Path Function (4 Magnet Chicane)

$\phi := \frac{0.5}{10} \quad Lb := 0.5 \quad L0 := 5.0 \quad Li := 1.0 \quad R0 := \frac{Lb}{\phi} \quad R0 = 10$

$X_0 := \begin{pmatrix} 0 \\ 0 \end{pmatrix} \quad s_0 := 0 \quad E_0 := \begin{pmatrix} 1 \\ 0 \end{pmatrix} \quad M := \begin{pmatrix} 1 & 0 \\ 0 & -1 \end{pmatrix}$

$X_1 := X_0 + R0 \cdot \begin{pmatrix} \sin(\phi) \\ 1 - \cos(\phi) \end{pmatrix} \quad s_1 := s_0 + Lb \quad E_1 := \begin{pmatrix} \cos(\phi) \\ \sin(\phi) \end{pmatrix}$

$X_2 := X_1 + L0 \cdot E_1 \quad s_2 := s_1 + L0 \quad E_2 := E_1$

$X_3 := X_2 + (X_1 - X_0) \quad s_3 := s_2 + Lb \quad E_3 := E_0$

$X_4 := X_3 + Li \cdot E_3 \quad s_4 := s_3 + Li \quad E_4 := E_0$

$X_5 := X_4 + M \cdot (X_1 - X_0) \quad s_5 := s_4 + Lb \quad E_5 := M \cdot E_1$

$X_6 := X_5 + L0 \cdot E_5 \quad s_6 := s_5 + L0 \quad E_6 := E_5$

$X_7 := X_6 + M \cdot (X_1 - X_0) \quad s_7 := s_6 + Lb \quad E_7 := E_0$

$R_s(S) :=$
- $j \leftarrow -1$
- for $i \in 0..7$: $j \leftarrow i$ if $(S > s_i)$
- $\begin{pmatrix} S \\ 0 \end{pmatrix}$ if $j = -1$
- otherwise:
  - $X_j + E_j \cdot (S - s_j)$ if $\mathrm{mod}(j,2) = 1$
  - otherwise:
    - $ic \leftarrow \left((1 \;\; 0 \;\; -1 \;\; 0 \;\; -1 \;\; 0 \;\; 1)^T\right)_j$
    - $\phi 0 \leftarrow \mathrm{atan}\left[\frac{(E_j)_1}{(E_j)_0}\right]$
    - $\phi \leftarrow \phi 0 + \frac{S - s_j}{R0} \cdot ic$
    - $X_j + R0 \cdot ic \cdot \begin{pmatrix} \sin(\phi) - \sin(\phi 0) \\ \cos(\phi 0) - \cos(\phi) \end{pmatrix}$

$U_s(S) :=$
- $j \leftarrow -1$
- for $i \in 0..7$: $j \leftarrow i$ if $(S > s_i)$
- $\begin{pmatrix} 1 \\ 0 \end{pmatrix}$ if $j = -1$
- otherwise:
  - E_j if $\mathrm{mod}(j,2) = 1$
  - otherwise:
    - $ic \leftarrow \left((1 \;\; 0 \;\; -1 \;\; 0 \;\; -1 \;\; 0 \;\; 1)^T\right)_j$
    - $\phi 0 \leftarrow \mathrm{atan}\left[\frac{(E_j)_1}{(E_j)_0}\right]$
    - $\phi \leftarrow \phi 0 + \frac{S - s_j}{R0} \cdot ic$
    - $\begin{pmatrix} \cos(\phi) \\ \sin(\phi) \end{pmatrix}$

next_arc function: this function is needed for observer positions on a line;
the line-section with the observer can be excluded from the integration range;
(the kernel function K is zero for the line-section with the observer;)

$$\text{next\_arc}(s_o) := \begin{cases} s_o \\ s_1 \text{ if } (s_1 < s_o)\cdot(s_o < s_2) \\ s_3 \text{ if } (s_3 < s_o)\cdot(s_o < s_4) \\ s_5 \text{ if } (s_5 < s_o)\cdot(s_o < s_6) \\ s_7 \text{ if } (s_7 < s_o) \end{cases}$$

$$S := 0, 0.01 .. s_7$$

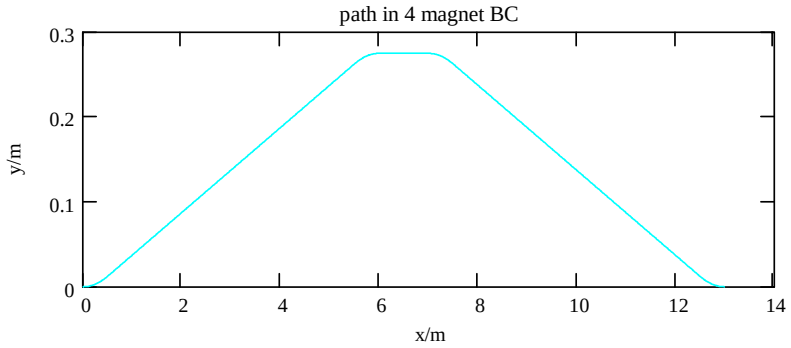

4. Time Mesh

$$t_a := -20\cdot\frac{\sigma_\lambda}{v} \qquad t_b := 5\cdot\frac{\sigma_\lambda}{v} \qquad N := 250 \qquad n := 0 .. N \qquad t_n := t_a + (t_b - t_a)\cdot\frac{n}{N}$$

5. Linear Motion Part

$$Q := \begin{pmatrix} -1.26551223 \\ 1.00002368 \\ 0.37409196 \\ 0.09678418 \\ -0.18628806 \\ 0.27886807 \\ -1.13520398 \\ 1.48851587 \\ -0.82215223 \\ 0.17087277 \end{pmatrix}$$

eerfc(x) = (1-erf(x))*exp(x^2):

$$\text{eerfc}(x) := \begin{cases} \dfrac{1}{\sqrt{\pi\cdot(0.5 + x^2)}} \text{ if } |x| > 1400 \\ \text{otherwise} \\ \quad t \leftarrow \dfrac{1}{1 + 0.5\cdot|x|} \\ \quad h \leftarrow 0 \\ \quad \text{for } n \in 9, 8 .. 0 \\ \quad\quad h \leftarrow Q_n + t\cdot h \\ \quad t\cdot\exp(h) \end{cases}$$

$$F(x) := \sqrt{\frac{\pi}{2}}\cdot\left(\text{eerfc}\left(\frac{x}{\sqrt{2}}\right)\right) \qquad gs(x) := \frac{-x}{\sqrt{2\cdot\pi}}\cdot e^{\frac{-x^2}{2}}$$

$$\text{split}(a,b,\Delta) := \left| \begin{array}{l} S \leftarrow (a \quad b)^T \\ n \leftarrow 2 \\ \text{for } i \in 0..\text{length}(\Delta) - 1 \\ \quad \text{if } (a < \Delta_i)\cdot(\Delta_i < b) \\ \quad\quad \left| \begin{array}{l} S_n \leftarrow \Delta_i \\ n \leftarrow n + 1 \end{array} \right. \\ \text{csort}(S,0) \end{array} \right.$$

this function is used to split the integration range

$$\text{Min}(a,b) := \left| \begin{array}{ll} a & \text{if } a < b \\ b & \text{otherwise} \end{array} \right.$$

$$E_{li}(t) := \left| \begin{array}{l} S \leftarrow \text{split}\left(-5 - \frac{v\cdot t}{\sigma_\lambda}, 5 - \frac{v\cdot t}{\sigma_\lambda}, \frac{\sigma_\eta}{\gamma\cdot\sigma_\lambda}\cdot 5\cdot(-1 \quad 1)^T\right) \\ X \leftarrow 0 \\ \text{for } n \in 0..\text{length}(S) - 2 \\ \quad X \leftarrow X + \int_{S_n}^{S_{n+1}} gs\left(x - \frac{v\cdot t}{\sigma_\lambda}\right)\cdot F\left(x\cdot\gamma\cdot\frac{\sigma_\lambda}{\sigma_\eta}\right) dx \\ \frac{-q_0}{4\cdot\pi\cdot\varepsilon_0\cdot\gamma\cdot\sigma_\lambda\cdot\sigma_\eta}\cdot X \end{array} \right.$$

calculation of linear motion field

$$eli_n := E_{li}(t_n)$$

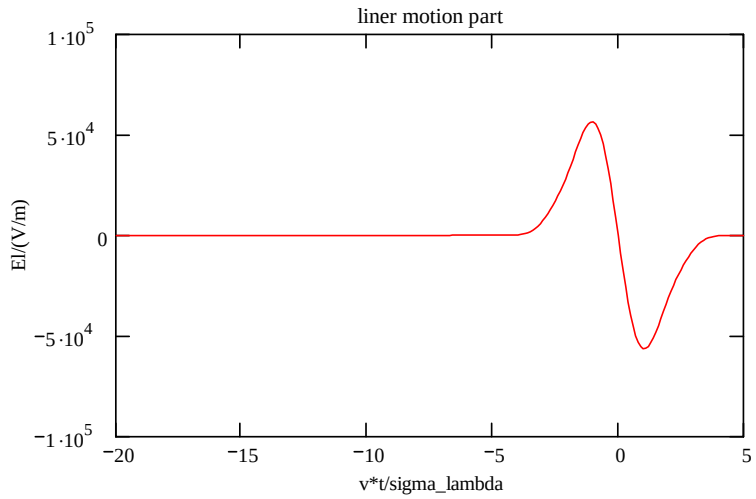

6. E123-Part

a) some functions

distance function: $R(s_o, s) :=$ RR ← $R_s(s_o) - R_s(s_o + s)$; $|RR|$

solve implicit equation s+beta*R(so,s)=u:
(needed for integration range)

step := 0.5 acc := $0.01 \cdot \sigma_\lambda$

```
s_of_u(so, u) :=
    sa ← 0
    if sa + β·R(so, sa) < u
        sb ← sa + step
        while sb + β·R(so, sb) < u
            sa ← sb
            sb ← sa + step
    otherwise
        sb ← sa
        while sa + β·R(so, sa) > u
            sb ← sa
            sa ← sb − step
            step ← 2·step
    while sb − sa > acc
        s ← 0.5·(sa + sb)
        sb ← s  if s + β·R(so, s) > u
        sa ← s  otherwise
    0.5·(sa + sb)
```

Kernel Eq.(16a): $sn := -50 \cdot \sigma_\lambda$ approximation for s>sn: R=-s, gamma^2*|s+beta*R|=-s

$K(s_o, s, r_o, u_o) :=$

$r_s \leftarrow R_s(s_o + s)$

$u_s \leftarrow U_s(s_o + s)$

$n \leftarrow r_o - r_s$

$R \leftarrow |n|$

if $R > 10^{-50}$

$n \leftarrow \frac{n}{R}$

$\frac{\beta \cdot \left[(n)^T \cdot (u_s - u_o) \right]_0 - \beta^2 \cdot \left[1 - \left((u_s)^T \cdot u_o \right)_0 \right] - \gamma^{-2}}{R} + \frac{1 - \beta \cdot \left((n)^T \cdot u_s \right)_0}{\gamma^2 \cdot |s + \beta \cdot R|}$ if $s < sn$

$\frac{\beta \cdot \left[1 - \left((n)^T \cdot u_o \right)_0 \right] - \beta^2 \cdot \left[1 - \left((u_s)^T \cdot u_o \right)_0 \right]}{-s}$ otherwise

0 otherwise

b) integration $TOL := 10^{-6}$

$$E_{l23}(s_o, t) := \begin{cases} 0 \text{ if } s_o \le 0 \\ \text{otherwise} \\ \quad s_l \leftarrow \text{Min}(0, s\_of\_u(s_o, v\cdot t - s_o - 5\cdot\sigma_\lambda)) \\ \quad s_u \leftarrow \text{Min}(0, s\_of\_u(s_o, v\cdot t - s_o + 5\cdot\sigma_\lambda)) \\ \quad s_n \leftarrow \text{next\_arc}(s_o) - s_o \\ \quad 0 \text{ if } s_n < s_l \\ \quad \text{otherwise} \\ \quad\quad s_u \leftarrow s_n \text{ if } s_n < s_u \\ \quad\quad r_o \leftarrow R_s(s_o) \\ \quad\quad u_o \leftarrow U_s(s_o) \\ \quad\quad S \leftarrow \text{split}(s_l, s_u, s - s_o) \\ \quad\quad X \leftarrow 0 \\ \quad\quad \text{for } n \in 0 .. \text{length}(S) - 2 \\ \quad\quad\quad X \leftarrow X + \int_{S_n}^{S_{n+1}} \lambda s(s + \beta\cdot R(s_o, s) + s_o - v\cdot t)\cdot K(s_o, s, r_o, u_o)\, ds \\ \quad\quad \frac{X}{4\cdot\pi\cdot\varepsilon_0} \end{cases}$$

$s_{oa} := 0.45$ $\quad ea_n := E_{l23}\left(s_{oa}, \frac{s_{oa}}{v} + t_n\right) + eli_n$ $\quad s_{ob} := s_{oa} + 5.5$ $\quad eb_n := E_{l23}\left(s_{ob}, \frac{s_{ob}}{v} + t_n\right) + eli_n$

$s_{oc} := s_{oa} + 7$ $\quad ec_n := E_{l23}\left(s_{oc}, \frac{s_{oc}}{v} + t_n\right) + eli_n$ $\quad s_{od} := s_{oa} + 12.5$ $\quad ed_n := E_{l23}\left(s_{od}, \frac{s_{od}}{v} + t_n\right) + eli_n$

observer position: 5cm before end of magnet
magnet 1, magnet 2, magnet 3, magnet 4

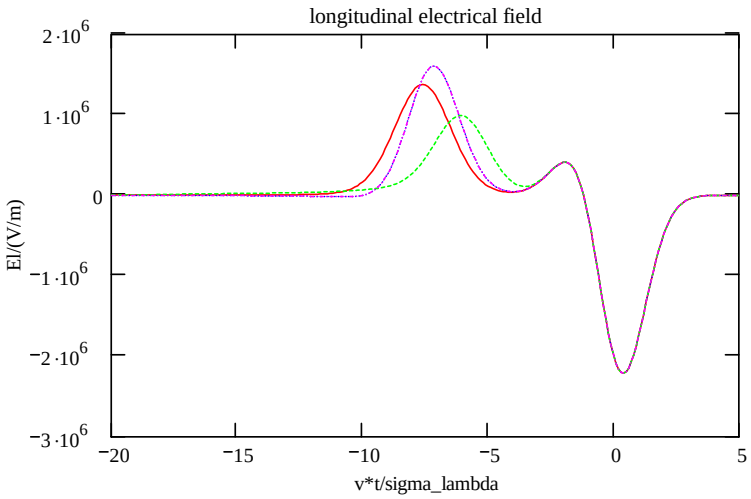

Appendix 2: Liénard-Wiechert Equation for the Electric Field

The electric field of a spherical Gaussian bunch in general motion can be calculated by a one-dimensional integration:

$$\mathbf{E}(\mathbf{r},t)=\frac{q}{\varepsilon(2\pi)^{3/2}\sigma^3}\left(\int_0^\infty((\mathbf{n}\cdot\boldsymbol{\beta})\boldsymbol{\beta}-\mathbf{n})\,\tilde{f}(\cdots)dr'-\frac{\sigma}{c^2}\int_0^\infty\dot{\mathbf{v}}\,f(\cdots)dr'\right).$$

For outlying observers (that are sufficiently separated from the source distribution) the auxiliary functions $f(a,b)$, $\tilde{f}(a,b)$ can be approximated by Gaussian normal distributions:

$$f(a,b)\to\sqrt{\frac{2}{\pi}}\frac{1}{b}g(a-b)\ ,$$

$$\tilde{f}(a,b)\to-\sqrt{\frac{2}{\pi}}\frac{1}{b}\left(g'(a-b)+\frac{1}{b}g(a-b)\right).$$

With the gaussian function $g^{(\sigma)}(x)=g(x/\sigma)/\sigma$ and its derivative $g'^{(\sigma)}(x)$ the electric field can be written as

$$\mathbf{E}(\mathbf{r},t)\to\frac{q}{4\pi\varepsilon}\int_{r'_l}^{r'_u}\left(\frac{\mathbf{n}-(\mathbf{n}\cdot\boldsymbol{\beta})\boldsymbol{\beta}}{\mathrm{R}}\left(g'^{(\sigma)}(r'-R)\right)+\left(\frac{\mathbf{n}-(\mathbf{n}\cdot\boldsymbol{\beta})\boldsymbol{\beta}}{\mathrm{R}^2}-\frac{\dot{\boldsymbol{\beta}}}{cR}\right)g^{(\sigma)}(r'-R)\right)dr'\ .$$

For point particles ($\sigma\to 0$) the Gaussian functions are substituted by Dirac distributions:

$$\mathbf{E}(\mathbf{r},t)\to\frac{q}{4\pi\varepsilon}\int_{r'_l}^{r'_u}\left(\frac{\mathbf{n}-(\mathbf{n}\cdot\boldsymbol{\beta})\boldsymbol{\beta}}{\mathrm{R}}\left(\delta'(r'-R)\right)+\left(\frac{\mathbf{n}-(\mathbf{n}\cdot\boldsymbol{\beta})\boldsymbol{\beta}}{\mathrm{R}^2}-\frac{\dot{\boldsymbol{\beta}}}{cR}\right)\delta(r'-R)\right)dr'\ .$$

The following properties are used for the integration of the Dirac function:

$$\int Q(\cdots)\delta(r'-R)dr'=\left(\frac{Q(\cdots)}{1-\mathbf{n}\cdot\boldsymbol{\beta}}\right)_{r'}$$

$$\int Q(\cdots)\delta'(r'-R)dr'=\left(\frac{-1}{1-\mathbf{n}\cdot\boldsymbol{\beta}}\frac{\partial}{\partial r'}\left(\frac{Q(\cdots)}{1-\mathbf{n}\cdot\boldsymbol{\beta}}\right)\right)_{r'}$$

with r' the solution of the implicit equation $r' = R(r', \mathbf{r}, t)$. Therefore the electric field is:

$$\mathbf{E}(\mathbf{r},t) \to \frac{q}{4\pi\varepsilon}\left(\frac{-1}{1-\mathbf{n}\cdot\boldsymbol{\beta}}\frac{\partial}{\partial r'}\left(\frac{\mathbf{n}-(\mathbf{n}\cdot\boldsymbol{\beta})\boldsymbol{\beta}}{(1-\mathbf{n}\cdot\boldsymbol{\beta})R}\right)+\left(\frac{\mathbf{n}-(\mathbf{n}\cdot\boldsymbol{\beta})\boldsymbol{\beta}}{R^2(1-\mathbf{n}\cdot\boldsymbol{\beta})}-\frac{\dot{\boldsymbol{\beta}}}{cR(1-\mathbf{n}\cdot\boldsymbol{\beta})}\right)\right)_{r'} .$$

The following r' derivatives are used

$$\partial_{r'}R(r',\mathbf{r},t) = \mathbf{n}\cdot\boldsymbol{\beta}$$

$$\partial_{r'}\mathbf{n}(r',\mathbf{r},t) = \frac{\boldsymbol{\beta}-\mathbf{n}((\mathbf{n}\cdot\boldsymbol{\beta}))}{R}$$

$$\partial_{r'}\boldsymbol{\beta}(r',\mathbf{r},t) = -\frac{\dot{\boldsymbol{\beta}}}{c}$$

$$\frac{\partial}{\partial r'}\left(\frac{\mathbf{n}-(\mathbf{n}\cdot\boldsymbol{\beta})\boldsymbol{\beta}}{(1-\mathbf{n}\cdot\boldsymbol{\beta})R}\right) = \frac{\mathbf{n}-(\mathbf{n}\cdot\boldsymbol{\beta})\boldsymbol{\beta}}{R^2}-\frac{(\mathbf{n}-\boldsymbol{\beta})}{\gamma^2R^2(1-\mathbf{n}\cdot\boldsymbol{\beta})^2}+\frac{\dot{\boldsymbol{\beta}}(\mathbf{n}\cdot\boldsymbol{\beta}-(\mathbf{n}\cdot\boldsymbol{\beta})^2)-(\mathbf{n}-\boldsymbol{\beta})(\mathbf{n}\cdot\dot{\boldsymbol{\beta}})}{cR(1-\mathbf{n}\cdot\boldsymbol{\beta})^2}$$

to simplify the expression for the electric field:

$$\mathbf{E}(\mathbf{r},t) \to \frac{q}{4\pi\varepsilon}\left(\frac{\mathbf{n}-\boldsymbol{\beta}}{\gamma^2\mathrm{R}^2(1-\mathbf{n}\cdot\boldsymbol{\beta})^3}+\frac{\mathbf{n}\times(\mathbf{n}-\boldsymbol{\beta})\times\dot{\boldsymbol{\beta}}}{cR(1-\mathbf{n}\cdot\boldsymbol{\beta})^3}\right)_{r'} .$$

Figures

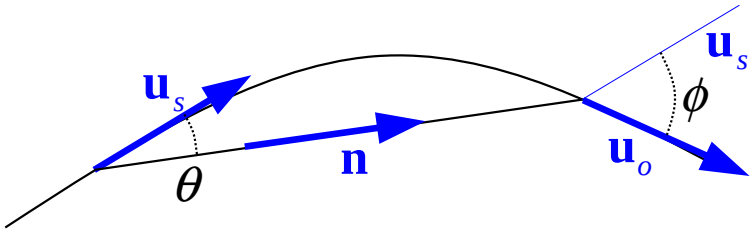

$$\mathbf{u}_s \cdot \mathbf{u}_o = \cos\phi \quad \mathbf{n} \cdot \mathbf{u}_s = \cos\theta \quad \mathbf{n} \cdot \mathbf{u}_o = \cos(\phi - \theta)$$

Fig. 1: Definition of angles ϕ and θ for planar path functions

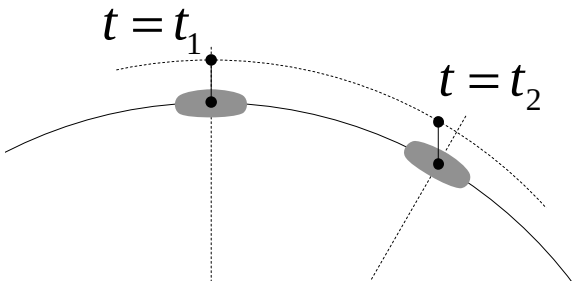

Fig. 2: The scalar potential for circular motion is not stationary for observer particles with offset.

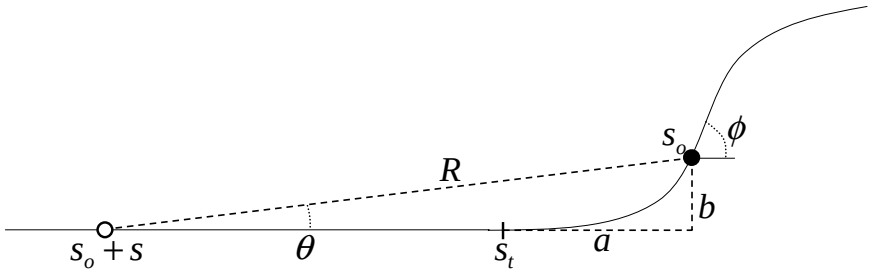

$$R = \sqrt{(a + s_t - (s_o + s))^2 + b^2} \qquad \theta = \arctan\frac{b}{a + s_t - (s_o + s)}$$

Fig. 3: Contribution from retarded Sources on a semi-infinite line $s_o + s < s_t$.

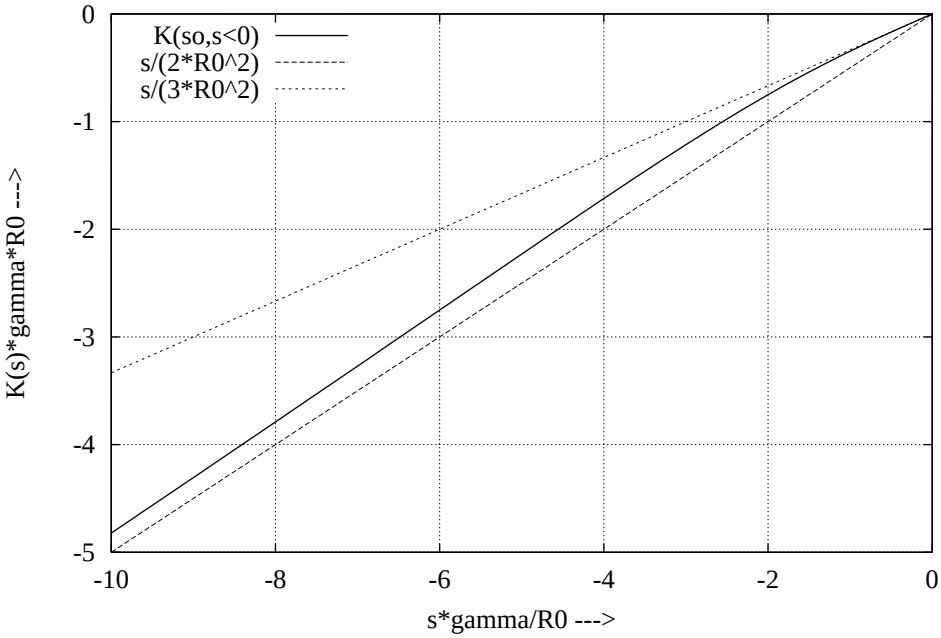

Fig. 4: Kernel $K(s_o, s < 0)$ for circular motion.

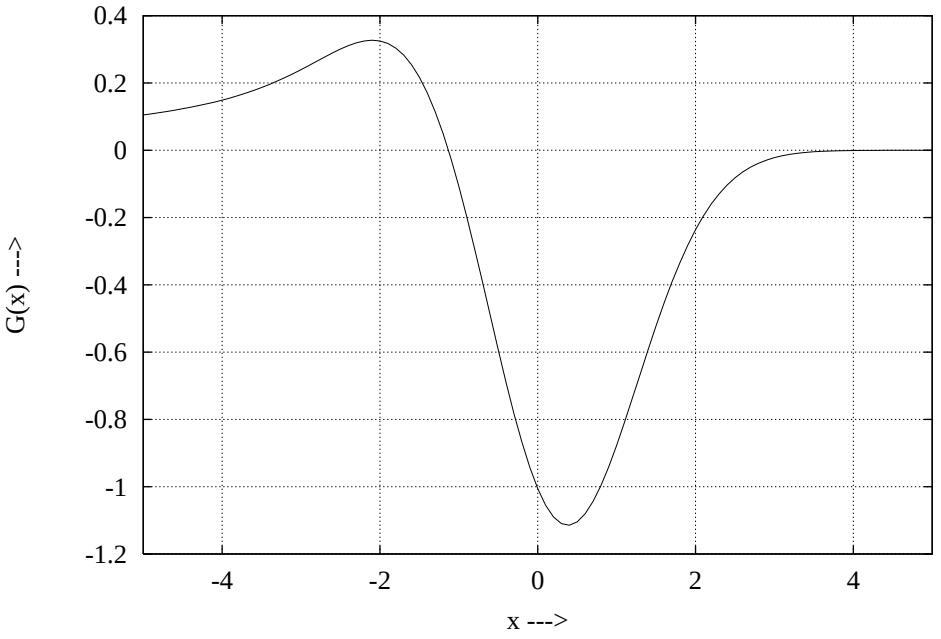

Fig. 5: Shape function $G(x)$ of Eq. (20). $G(x)$ describes the energy independent approximation of the normalized longitudinal field of a gaussian bunch in circular motion.

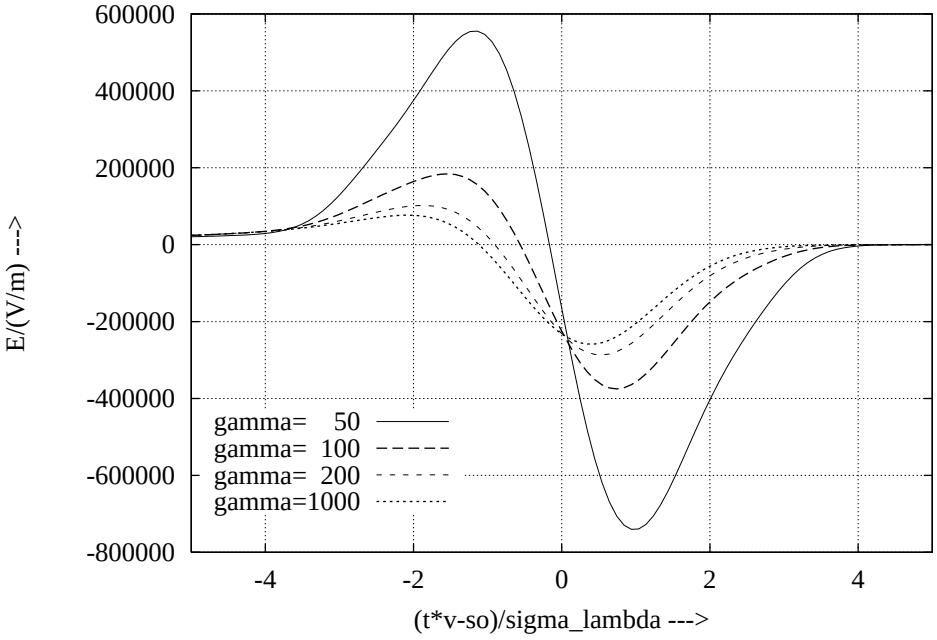

Fig. 6: Longitudinal field of a round gaussian bunch in circular motion, with $q = 1\,\mathrm{nC}$, $\sigma_\lambda = \sigma_\eta = 100\mu\mathrm{m}$, $R_0 = 10\,\mathrm{m}$ and $\gamma = 50, 100, 200, 1000$.

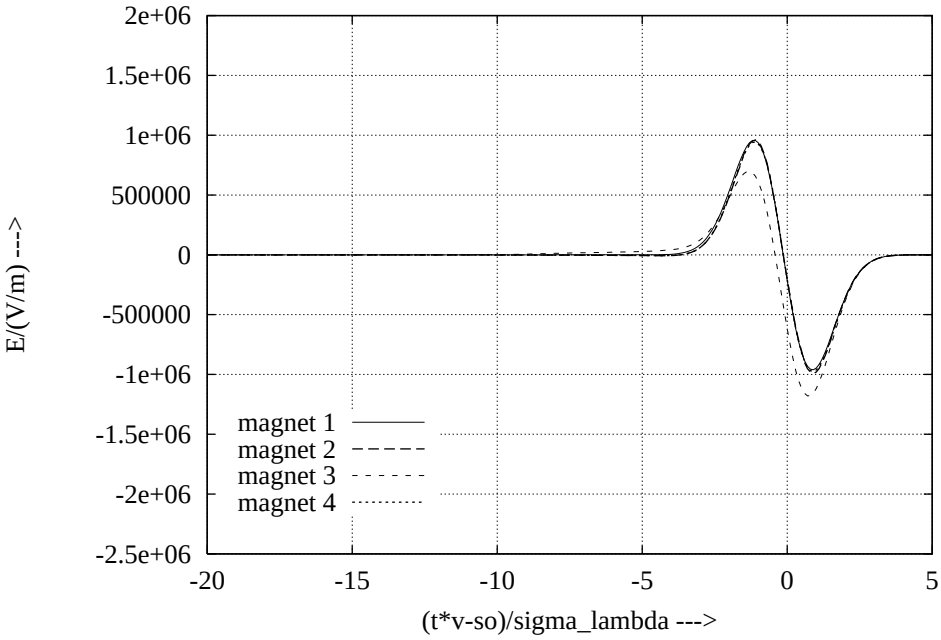

Fig. 7: Time dependent longitudinal field of a Gaussian bunch in a bunch compressor chicane. The fields are calculated for positions 15 cm after the entrance of the magnets.

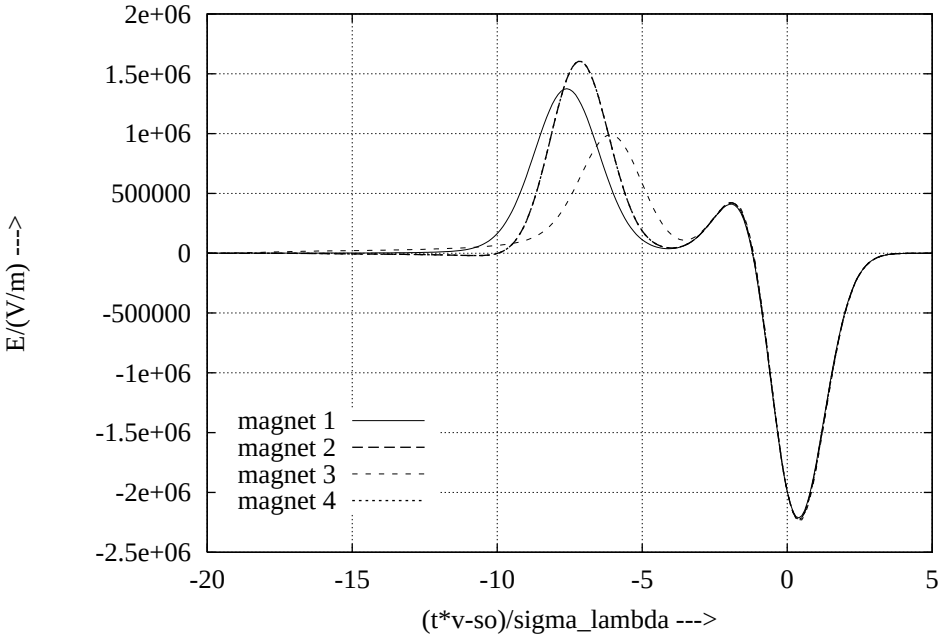

Fig. 8: Time dependent longitudinal field of a Gaussian bunch in a bunch compressor chicane. The fields are calculated for positions 45 cm after the entrance of the magnets. (Curves for magnet 2 and 4 are plotted on the same line.)

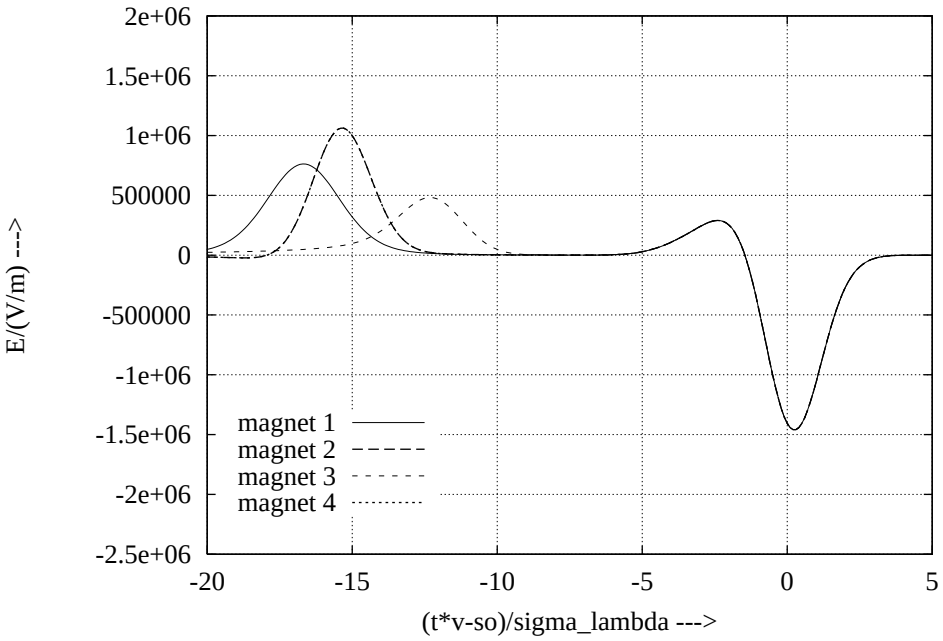

Fig. 9: Time dependent longitudinal field of a Gaussian bunch in a bunch compressor chicane. The fields are calculated for positions 10 cm after the exit of the magnets. (Curves for magnet 2 and 4 are plotted on the same line.)

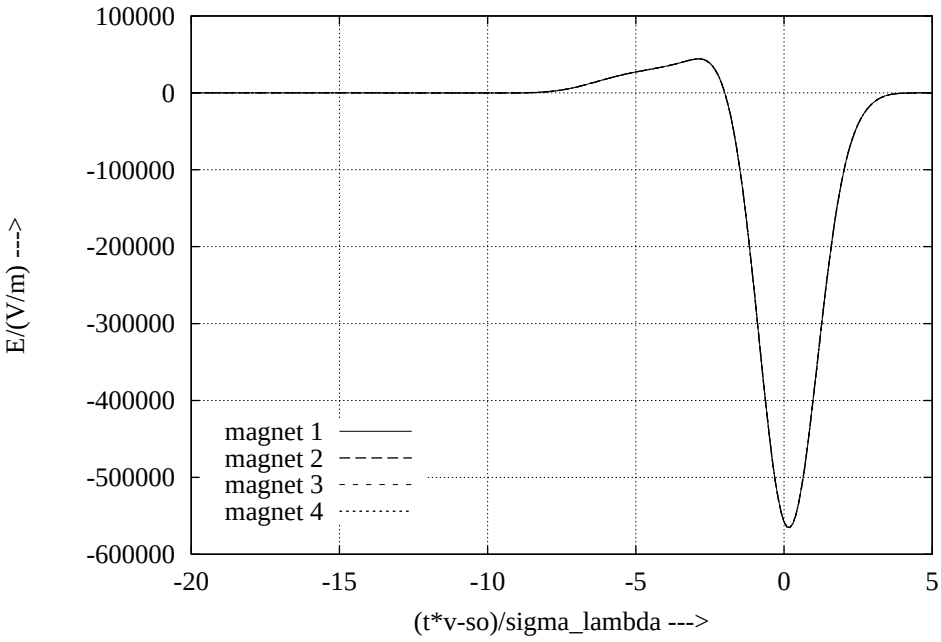

Fig. 10: Time dependent longitudinal field of a Gaussian bunch in a bunch compressor chicane. The fields are calculated for positions 50 cm after the exit of the magnets.

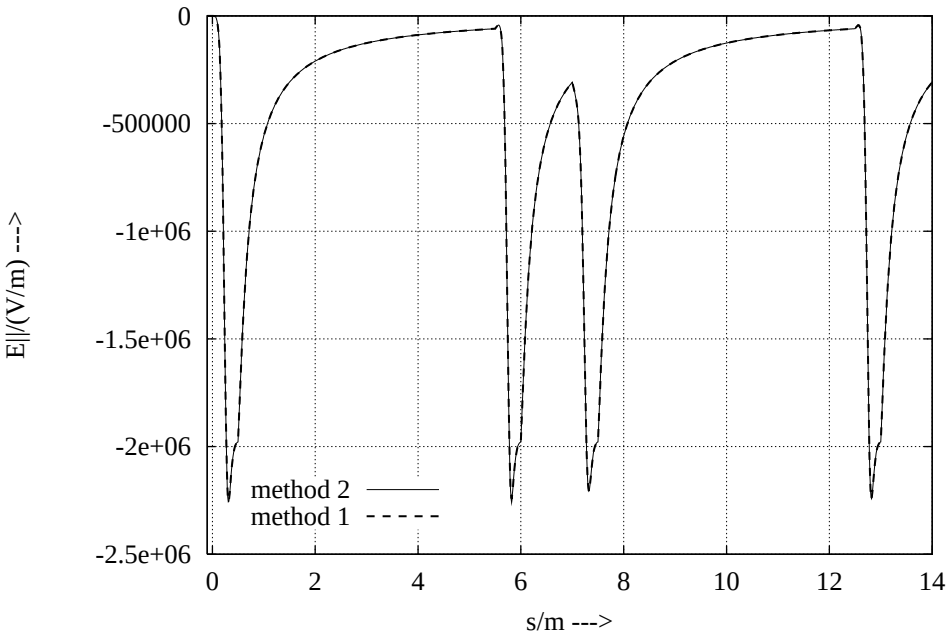

Fig. 11: Longitudinal electric field in the center of a spherical Gaussian bunch that travels through a bunch compressor chicane. The field is plotted as a function of the position in the chicane.

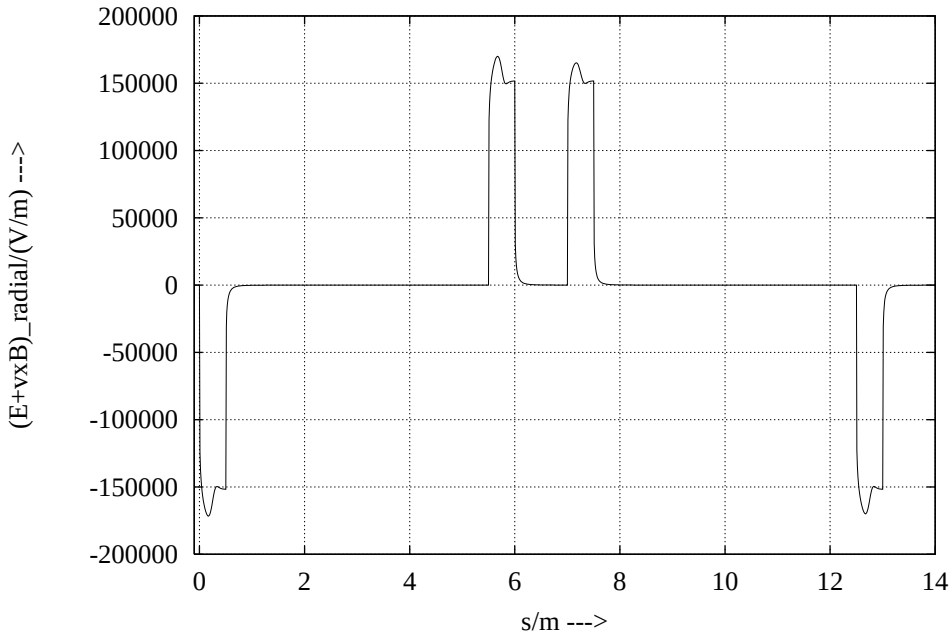

Fig. 12: Transverse component of the Lorentz force $(\mathbf{E}+\mathbf{v}\times\mathbf{B})\cdot\mathbf{u}_{\perp}$ in the center of a spherical Gaussian bunch that travels through a bunch compressor chicane.

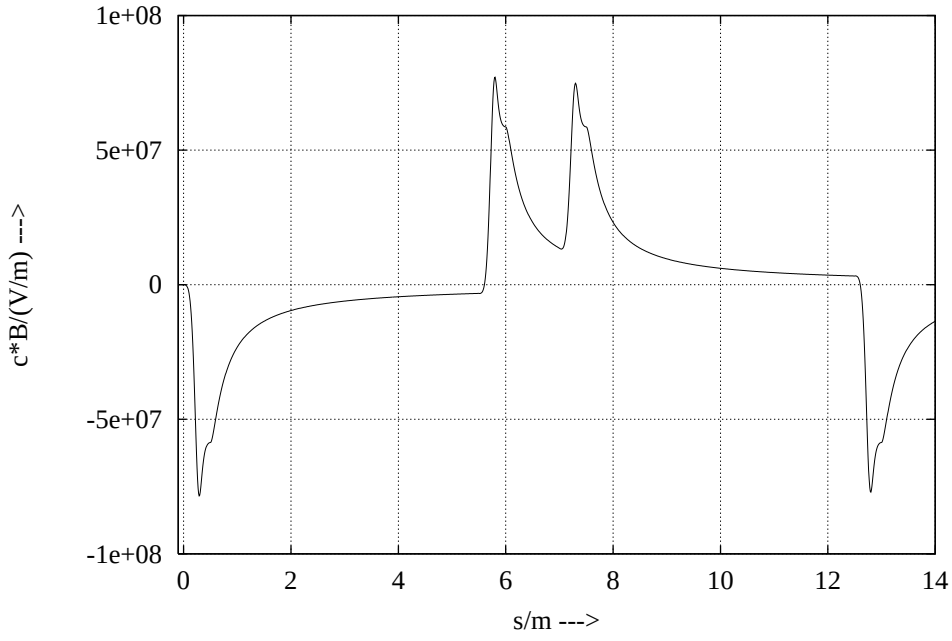

Fig. 13: Magnetic field in the center of a spherical Gaussian bunch that travels through a bunch compressor chicane. (The magnetic field is perpendicular to the plane of motion.)

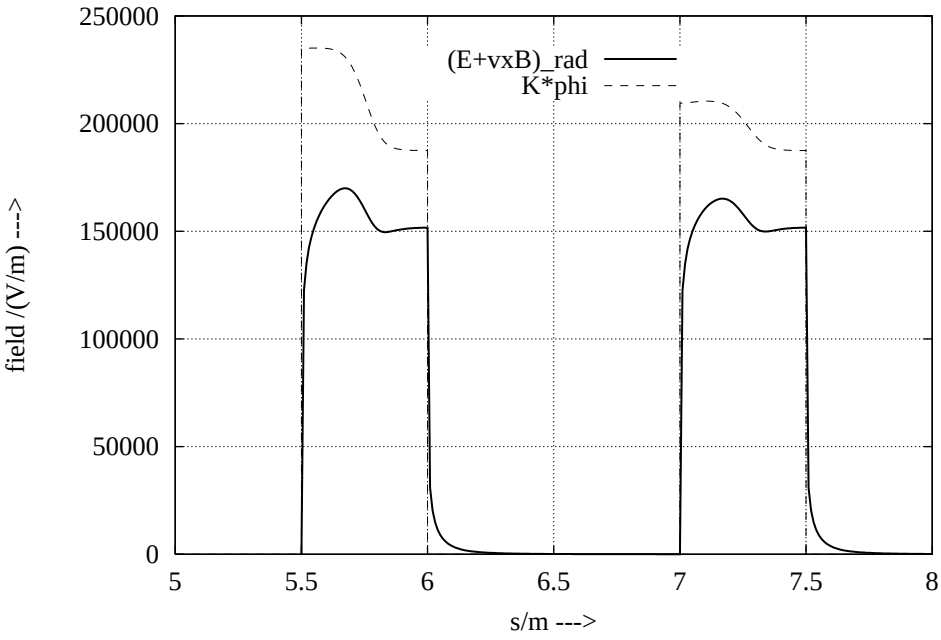

Fig. 14: Transverse force and scalar potential in the center of a spherical Gaussian bunch that travels through magnets 2 and 3. The scalar potential is multiplied by the inverse curvature radius.

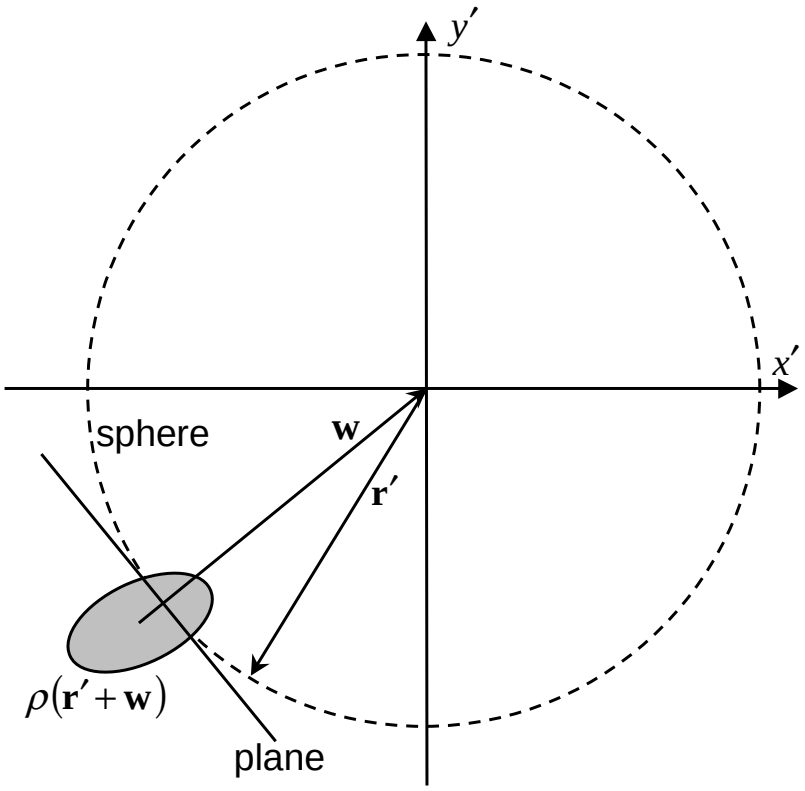

Fig. 15: Planar approximation: for large radius r' the spherical integration surface is replaced by a plane.

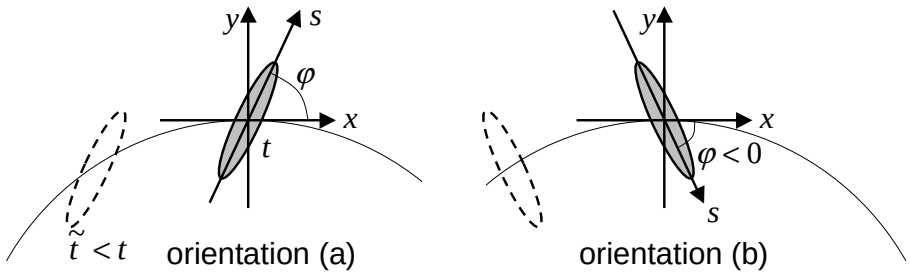

Fig. 16: Flat elliptical bunch in circular motion. The rms dimensions in s and z direction are $\sigma_s = \sigma_z = 500\,\mu$m. (The z-direction is perpendicular to the plane of motion.) The third rms dimension is $5\,\mu$m. The angle between the s and x direction is 87.78^o for orientation (a) and -87.78^o for orientation (b). The projected bunch length for both orientations is $20\,\mu$m. The radius of the circular trajectory and the Lorentz factor are $R_0 = 10$ m and $\gamma = 1000$.

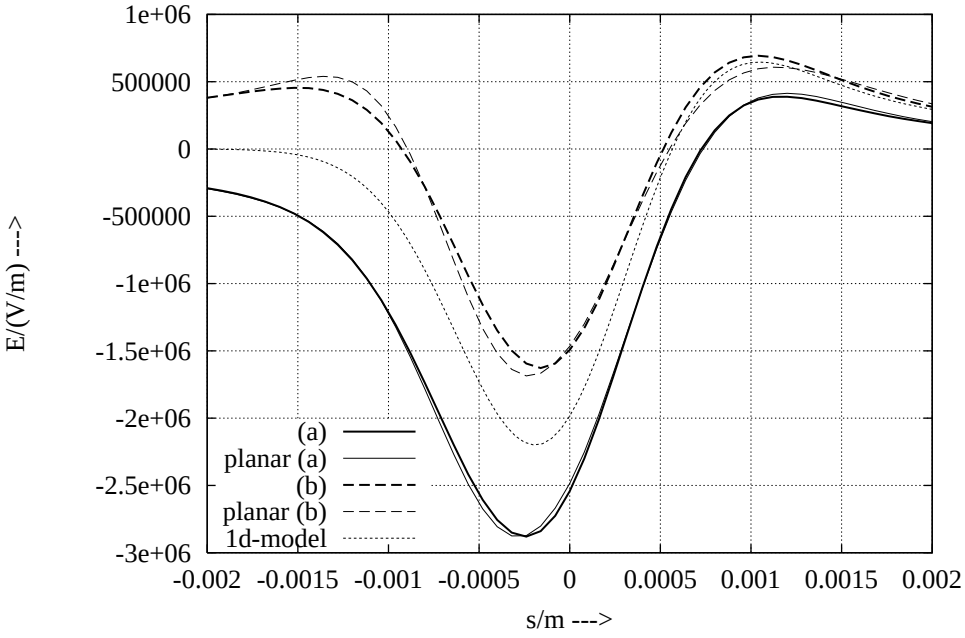

Fig. 17: Longitudinal field in a flat elliptical bunch for orientation (a) and (b) as shown in Fig. 16. Bunch charge $q = 1$ nC, thick lines: exact calculation, solid and dashes lines: planar approximation, dotted line: one-dimensional estimation by Eq. (20).

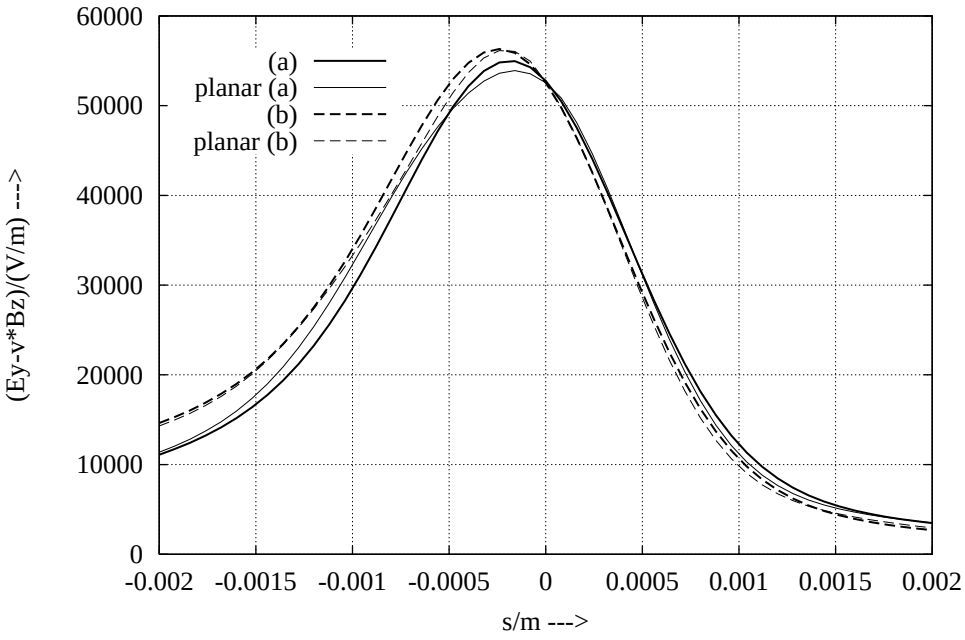

Fig. 18: y -component of the Lorentz force in a flat elliptical bunch for orientation (a) and (b) as shown in Fig. 16. Bunch charge $q = 1\,\mathrm{nC}$, thick lines: exact calculation, solid and dashes lines: planar approximation.